AD NUMBER

AD466558

NEW LIMITATION CHANGE

TO
 Approved for public release, distribution
 unlimited

FROM
 Distribution authorized to U.S. Gov't.
 agencies only; Administrative/Operational
 Use; May 1965. Other requests shall be
 referred to Air Force Dynamics Lab.,
 Wright-Patterson AFB, OH 45433.

AUTHORITY

AFFDL ltr, 29 Dec 1978

AFFDL-TR-65-41

OXIDATIVE DETONATIONS INITIATED BY HIGH VELOCITY IMPACTS

A. P. CARON

NORTHROP SPACE LABORATORIES

TECHNICAL REPORT AFFDL-TR-65-41

MAY 1965

OXIDATIVE DETONATIONS INITIATED BY HIGH VELOCITY IMPACTS

A. P. CARON

NORTHROP SPACE LABORATORIES

FOREWORD

This technical report has been reviewed and is approved.

RICHARD F. HOENER
Acting Chief
Structures Division

ii

ABSTRACT

Aluminum sheets (0.25 and 0.30 mm thick) retaining oxygen at one atmosphere have been observed to burst when impacted with steel and aluminum spheres (3.2 mm diameter) at velocities beyond 5.8 and 6.3 Km/sec, respectively. Visible deposits of aluminum and iron oxide, target sheet bulges, strong light intensities, and pressure gauge traces of detonation waves indicate that the bursting pressures were caused by the violent oxidation of steel and aluminum. Evidence of such reactions was detected over a wide range of impact velocities (4.88 to 8.02 Km/sec) and the violence of the reaction was found to be a function of the velocity. Other tests showed that both the projectile and the target participate in the formation of detonations and that other factors determining the strength of such detonations are the concentration of oxygen and the amount of impacted metal susceptible to oxidation.

TABLE OF CONTENTS

ILLUSTRATIONS

I. INTRODUCTION

The meteoroid hazard to aerospace vehicles has been a subject of concern
for some time. Most of the efforts to guard against such hazards have been
directed toward the minimization of meteoric penetration. It is recognized,
however, that the best practical wall structure will always be associated
with a small but finite penetration probability and, thus, it is important
and pertinent to study the consequences of meteoric penetrations. This is
particularly true if such consequences might be catastrophic as indicated by
some reports.

A limited amount of data has been reported on the effect of high velo-
city impacts on metal tanks retaining gaseous oxygen. Rolsten and Hunt
(References 1 and 2) have shown that explosions accompanied by bright flashes
are produced when titanium sheets retaining oxygen are impacted by steel pro-
jectiles with velocities between 1.8 and 4.6 Km/sec; in addition, the tita-
nium sheets are often severely consumed after such explosions.

Gell and co-workers (References 3 and 4) also observed brilliant flashes
on impacting aluminum sheets retaining gaseous oxygen at one atmosphere with
velocities of about 7.6 Km/sec. Such explosions were noted to cause hair and
skin burns as well as fatal lung damage to rats inside the tank.

At Northrop Space Laboratories, a self-sealing panel faced on both sides
with aluminum and retaining air was blown out by a violent explosion when
impacted by a steel projectile with a velocity of about 5.6 Km/sec. At lower
impact velocities, no such explosion was observed. Finally, no explosions
were noted at velocities as high as 8.0 Km/sec with similar panels so long as
they were faced with epoxy-glass laminates (Reference 5).

From the few results given above, it thus appears that under certain
ballistic conditions the following phenomena may occur as a consequence of
high velocity penetrations of gaseous oxygen tanks:

1. Violent explosions with possible severe damage to life inside the
    tank

2. The burning of large wall areas, or

3. The blowing out of the walls.

It is generally believed that these phenomena are a result of pyrophoric
oxidation reactions of the impacted projectile and wall material with gaseous
oxygen although the oxidation products have never been characterized or
detected. However, in a closely related series of experiments, the spectrum
of AlO, a high temperature form of aluminum oxide, was identified in the
visible range as a thick aluminum target was impacted in air at velocities of
about 2.4 Km/sec (Reference 6).

It is known that metals such as aluminum and titanium are susceptible to
oxidation; the free energies of the respective oxides are highly negative and
the reactions are exothermic (see Table 1). At room temperature, their rate

1

of oxidation is slow because they are diffusion controlled. However, at higher temperatures, these metals and others ignite spontaneously in oxygen (see Table 1).

It thus appears that, upon a high velocity impact, the target sheet and projectile are compressed to high pressures and temperatures (Reference 7). Subsequently, these shocked metals are projected in the gaseous oxygen where they expand into a cloud of finely dispersed metal which oxidizes rapidly and explodes.

As seen above, although the "pyrophoric" effect is not altogether unexplainable, very little experimental work has been carried out in this field and most of the details of the mechanism of this explosive oxidation are totally lacking in spite of its practical importance.

It was therefore believed worthwhile to investigate the "pyrophoric" effect (particularly that associated with aluminum) with the goal in mind to first delineate the problem, determine some of its main characteristics, and gain laboratory experience in order to build a good foundation for a more systematic and fundamental future study.

TABLE 1

OXIDATION PROPERTIES OF SELECTED METALS

METAL	APPROXIMATE IGNITION POINT ºC	OXIDATION		
		ΔH_{298} Kcal/mole of Metal	ΔF_{298} Kcal/mole of Metal	OXIDE
Be	--	-146	-139	BeO
Mg	623	-144	-136	MgO
Al	1000	-200	-188	Al_2O_3
Fe	930	-98	-88	Fe_2O_3
Ti	610	-226	-204	TiO_2

II. EXPERIMENTAL

A. Procedure

A light-gas gun owned and operated by the McGill Space Research Institute was used to impact thin target sheets with spheres. This gun has a bore of 12.7 mm (0.5-inch) and is fired with a black powder charge of 500 to 850 gr. and with hydrogen gas in the two pressure chambers. The projectiles were seated on full bore Lexan sabots. At the end of the evacuated barrel, the sabot and projectile were separated by a short travel in air at one atmosphere. Subsequently, the sabot was deflected by hitting a deflector plate while the projectile traveled about 3.7 m in a chamber evacuated to 3 mm Hg.

The velocity of the projectiles was accurately determined by the use of a counter triggered as the projectiles traversed a light screen and stopped as a vacuum phototube recorded the impact flash. The distance over which the projectiles were timed was 3.60 m. In order to determine whether the projectiles triggered the light screen properly, flash X-ray pictures of the projectile and sabot in fl' .ht were obtained for nearly every shot. In some instances where the sabot, rather than the projectile, triggered the light screen, corrections to the velocity could be made by noting their relative positions on the picture. Under these conditions, it is believed that the maximum error in the calculated velocities is no larger than $\pm$ 1%.

The target sheet was pressed on an O-Ring at the mouth of a heavy wall (8 mm thick) brass shock tube (see Figure 1). Along the side and at the end of the tube five photocells were inserted in holes spaced at known distances. The photocells (N-P-N diffused silicon photo-duo-diodes, Type 1N2175), manufactured by Texas Instruments, Inc., were operated with a bias voltage of 45 volts. They are reputed to have a rise time of 2 μsec. and although their fall time is claimed to be 45 μsec, from our experience, we have reason to suspect that the fall time may be longer and function of the maximum light intensity suffered. In many instances, the photocells were saturated by the light flashes inside the shock tube and no corrective measures were taken because it was judged impractical and unwarranted for this preliminary study. Vacuum phototubes with fast rise and fall times mounted externally on plexiglass windows would be much more suitable and reliable for a later study.

All five photocells were provided with slit holes: the four slit holes along the side of the shock tube had a diameter of 1.1 mm and a length of 6.5 mm while the one at the end of the tube had a diameter of 0.4 mm and a length of 2.5 mm. Such small slits and blackened shock tube walls insured that the photocells recorded only the intensity of a light source essentially on the axis of the slit holes; this was verified with the use of flash bulbs lit at the mouth of the shock tube. Also, in a number of tests, under certain specified conditions, strong signals could be detected at impact on the front side of the target sheet while little or no light signals were detected in the shock tube.

In addition, a pressure gauge was placed near the target sheet (5.1 cm) and mounted flush with the inside wall of the shock tube. At first a capacitance pressure gauge (Photocon Research Products, Model No. 402R) was used with a Dynagage system. It was later discovered, however, that the resonant

3
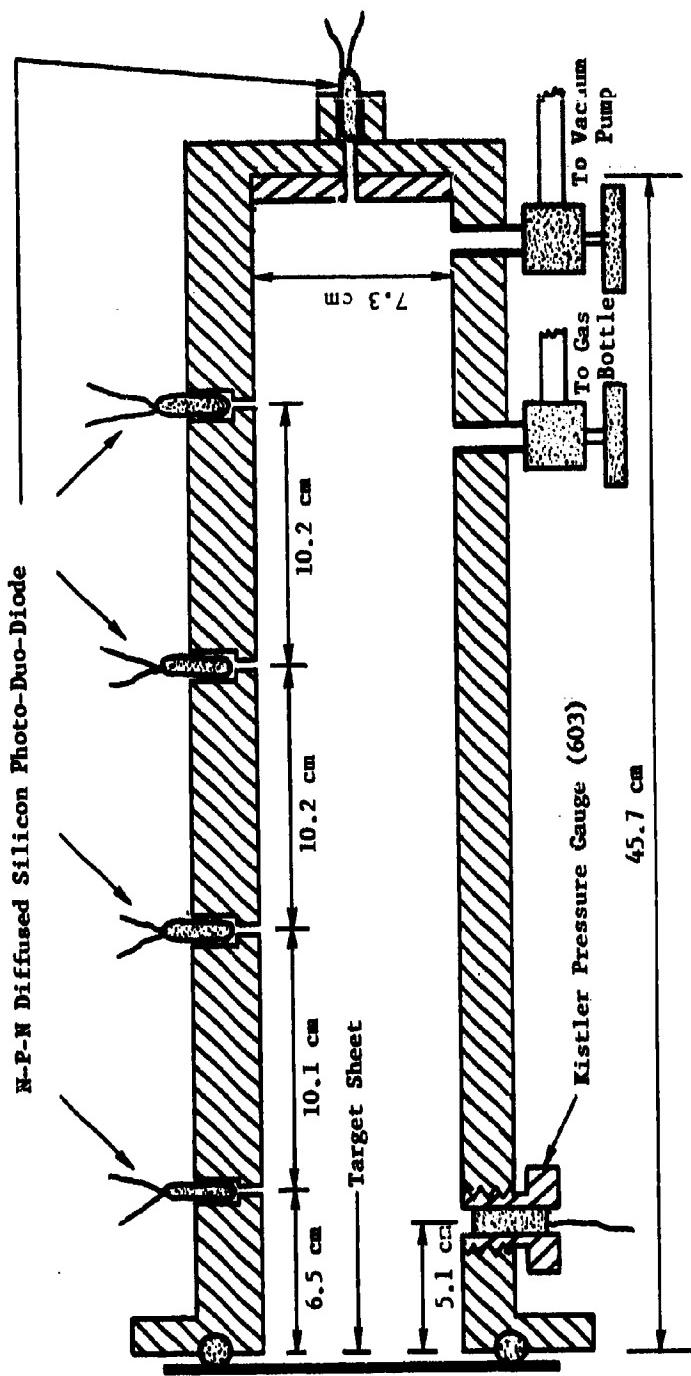
Figure 1. Shock Tube

4

frequency (12,000 cps) was too low for the short pressure pulses arising in the shock tube. As a consequence, a quartz Kistler gauge (Model 603) was substituted and found to be satisfactory (300,000 cps), although it was not reliably calibrated. Thus, the pressure data (recorded with the latter gauge) presented and discussed in the sections to follow are qualitative and only the recorded times of the pressure histories are quantitatively meaningful.

Finally, the shock tube was equipped with two valves and a pressure gauge. Prior to each high velocity impact, the tube was evacuated to about 75 mm Hg. and back filled with either gaseous oxygen or helium.

The projectiles had a diameter of 3.2 mm (1/8-inch) and were of the following composition:

1. 2017 Aluminum
2. High carbon chrome alloy steel
3. Pyrex
4. Quartz (ground crystal)
5. Synthetic cut sapphire

These last three types of projectiles were used in an attempt to impact oxidized materials. Unfortunately, flash X-ray pictures showed that all three fractured before impact. Thus, these materials could not survive the high acceleration of the light-gas gun.

The target sheets were of several types:

1. Aluminum 2024-T3 Alcoa, 0.25 mm (0.010-inch) thick
2. Aluminum 7075-T6 Alcoa, 0.30 mm (0.012-inch) thick
3. One-ply epoxy-fiberglas (12 parts DTA, 100 parts EPON 828, #181 Volan glass fiber), 0.37 mm (0.015-inch) thick.

B. Case I: Impact of Aluminum on Aluminum Sheets Retaining Oxygen at One Atmosphere

Fifteen aluminum sheets (12 sheets 0.25 mm thick and 3 sheets 0.30 mm thick) retaining oxygen at one atmosphere were impacted with aluminum spheres at velocities ranging from 4.91 to 8.02 Km/sec.

The following observations were made:

1. The target sheets and the walls of the shock tube were always coated after impact with a white powder which was not characterized but which, no doubt, is Al_2O_3.

2. The target sheets bulged outward to a degree which appears to be a function of velocity. At 6.16 and 6.26 Km/sec, petalling and a crack were observed while, at 6.31 Km/sec and beyond, the target sheets completely burst (see Figures 21 and 22, Appendix). Thus, the bursting velocity is estimated to be 6.3 Km/sec. Figures 2 and 3 show the dependence of the bulge depths and volumes (measured independently) on impact velocity.

5

Figure 2 Bulge Depth

(Aℓ or Aℓ, 1 atm. O$_2$)

6

Critical Bulge Volume

Bursting
Velocity

● Burst
◕ Extensive Petalling
◔ Small Cracks
◎ No Crack

Volume, cm³

4.6

4

3

2

4   5   6   6.3 7   8

Impact Velocity, Km/sec.
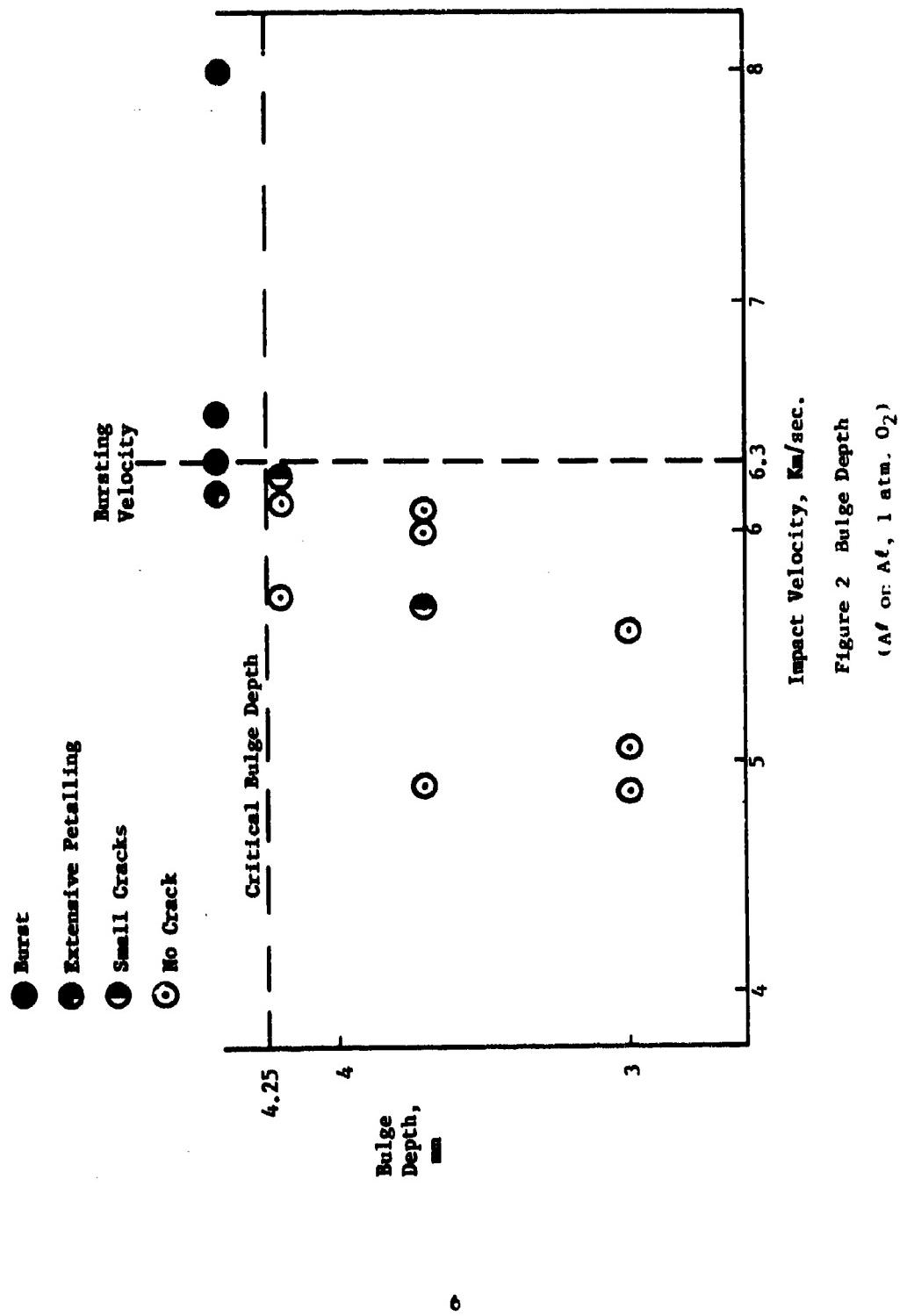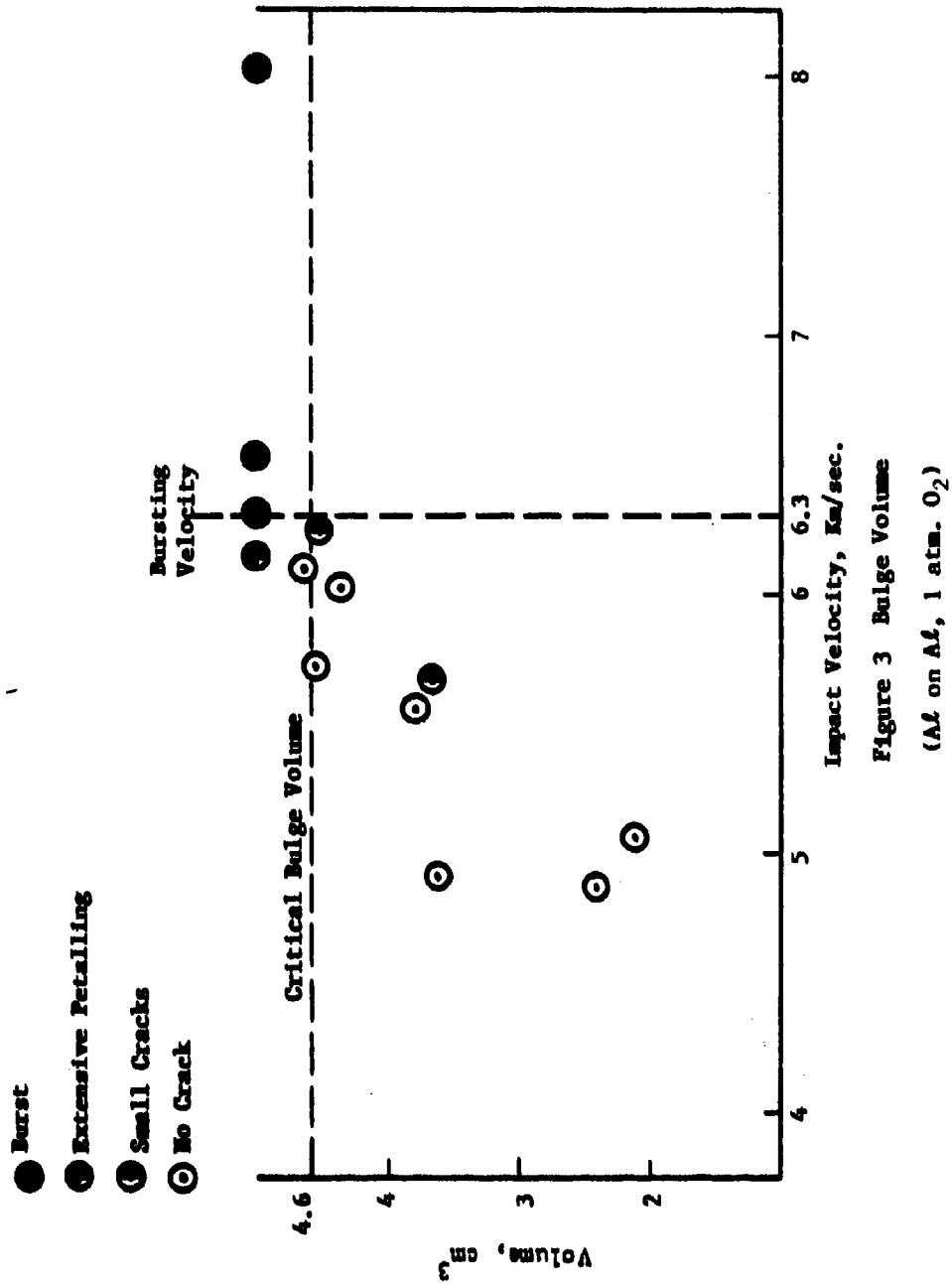
Figure 3 Bulge Volume

(Aℓ on Aℓ, 1 atm. O₂)

7

The shape of the bulges was observed to be perfectly symmetrical
with the maximum depth at the center of the sheet regardless of the
impact location. This indicates that the shock waves responsible
for the deformation had a diameter substantially equal to that of
the shock tube, that the waves were therefore essentially planar,
and that they originated at some distance (at least 7 cm) from the
target sheet.

3. Strong light intensities were recorded with the side photocells (see
   Figure 4) and the end photocell at all impact velocities. Unfortu-
   nately, no quantities may be ascribed to such intensities because in
   all instances the cells were saturated. However, the saturation
   times may be used as a rough measure of the intensity and Figure 5
   shows that these times do generally increase with the impact velo-
   city: this is particularly the case of the photocell nearest the
   target. Figure 6 shows how the light intensity decreases away from
   the target sheet.

4. It was noted that, after impact, the times to reach the saturation
   point increased as the photocell was further removed from the target
   sheet. The time lags were found to vary from 60 to 80 μsec and were
   used to calculate velocities which are shown on Figure 7 as a
   function of the impact velocity.

   It is believed that these velocities should represent the escape
   velocity (Reference 8) of the aluminum fragments since such frag-
   ments would be expected to be quite luminous from the exothermic
   oxidation taking place at their surface (Reference 9). It is un-
   likely that these velocities are associated with gaseous detonation
   waves because the magnitudes are too large and, as will be seen
   later, do not correspond to the values obtained from the pressure
   traces.

   For comparison purposes, a theoretical fragment escape velocity
   curve (shown on Figure 7) was computed with Hugoniot data compiled
   by Zwarts (1964). The experimental velocities are appreciably
   lower, and two causes are probably responsible for this discrepancy:

   (a) The lag times could not be based on the induction periods of
        the photocells because of the lack of time resolution. The
        measured lag times, based on the rise times to saturation, are
        longer and probably more representative of the velocity of the
        center of mass of the expanding aluminum cloud rather than the
        fragment escape velocity, a limiting velocity.

   (b) The fragment escape velocity computed is based on the assump-
        tion that the expansion takes place in vacuum. However, at a
        pressure of one atmosphere, the fragment escape velocity should
        be lower.

5. The pressure traces indicate that the aluminum oxidation takes place
   over times varying from 1 to 1.5 msec (see Figure 8). The pressure
   waves observed are typical of detonation waves, i.e., sharp pressure
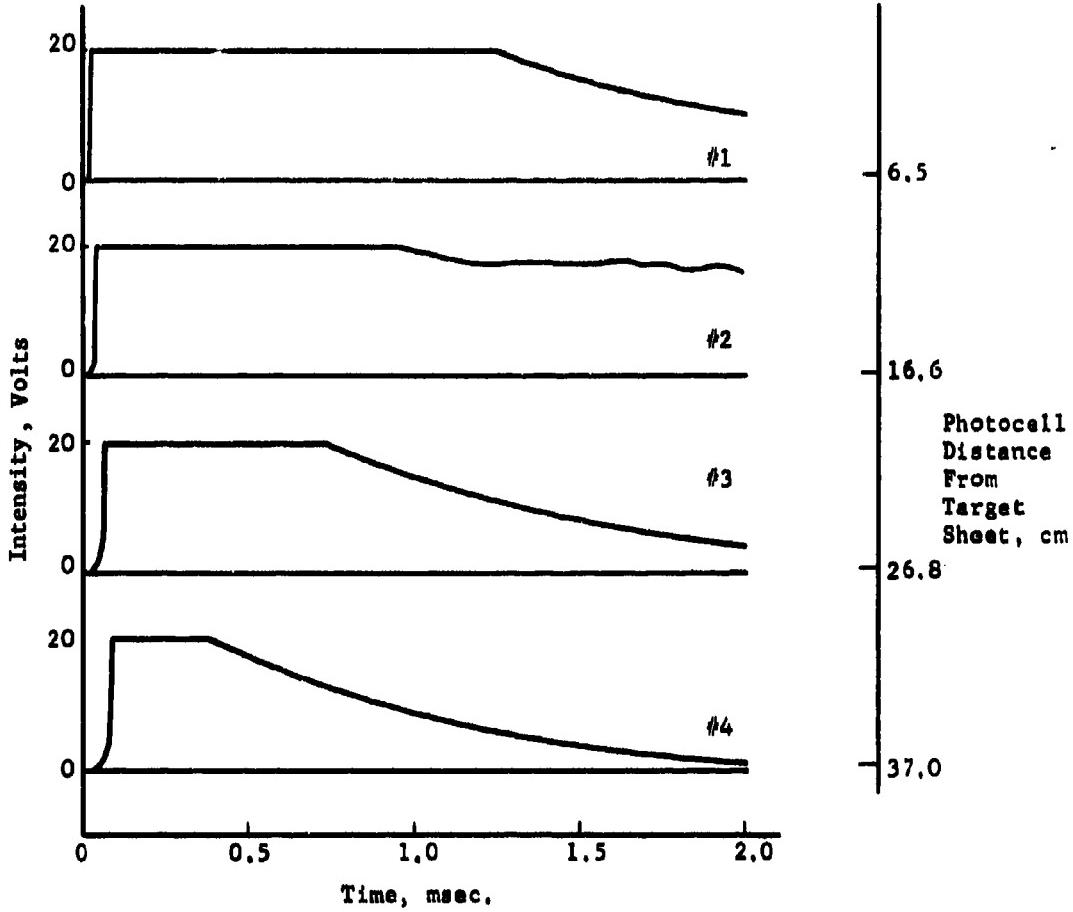
Figure 4 Typical Traces of Side Photocells for Al on Al with 1 atm. O_2
(Shot #1370, Impact Velocity: 6.02 Km/sec)

9
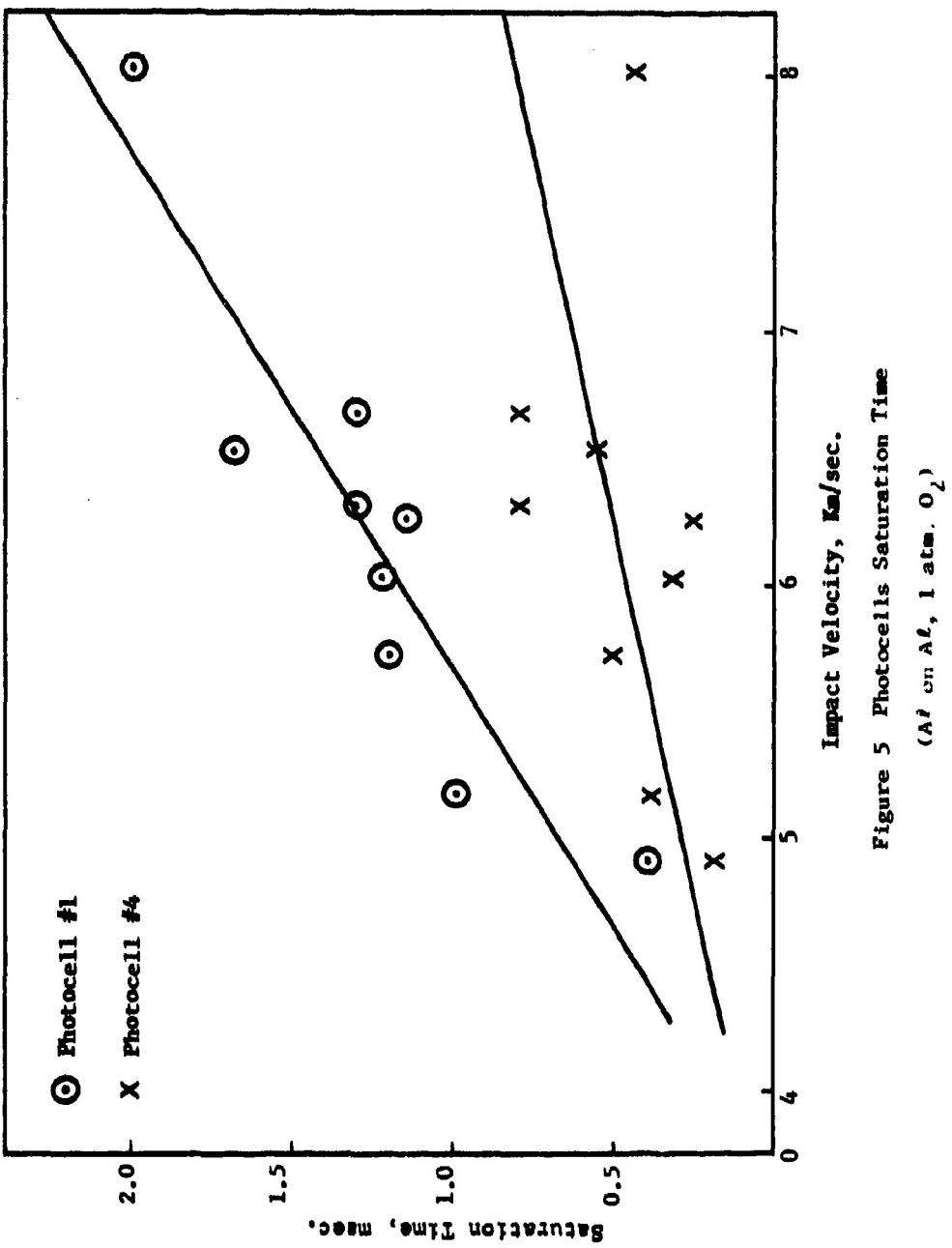
Figure 5 Photocells Saturation Time

(Aℓ on Aℓ, 1 atm. O₂)

10
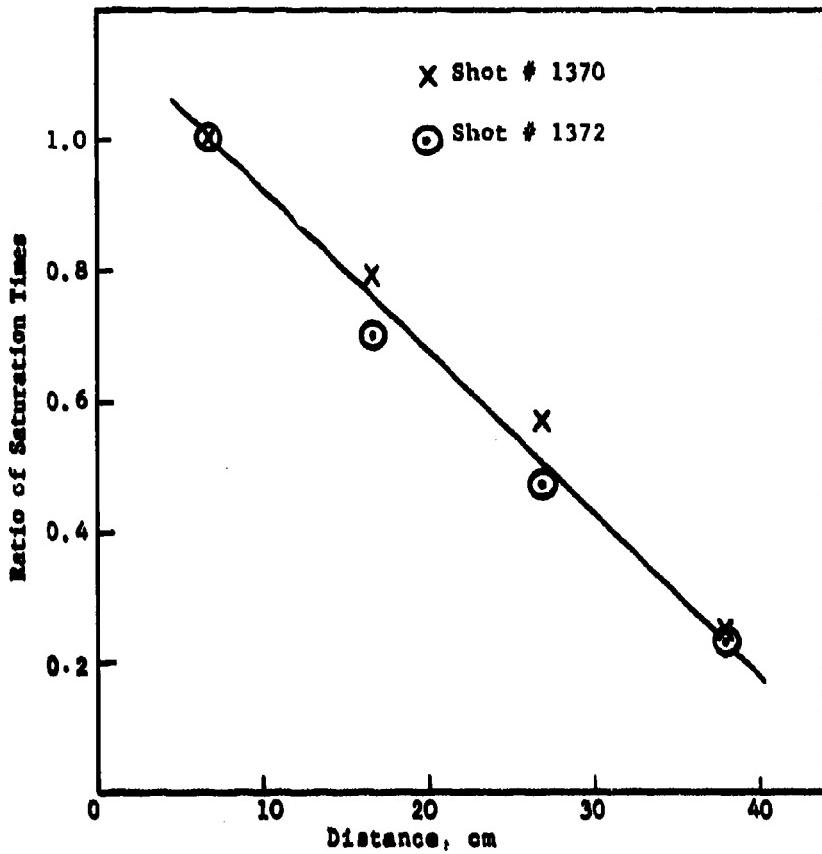
Figure 6 Ratio of Photocell Saturation Times

(Aℓ on Aℓ, 1 atm. O_2)
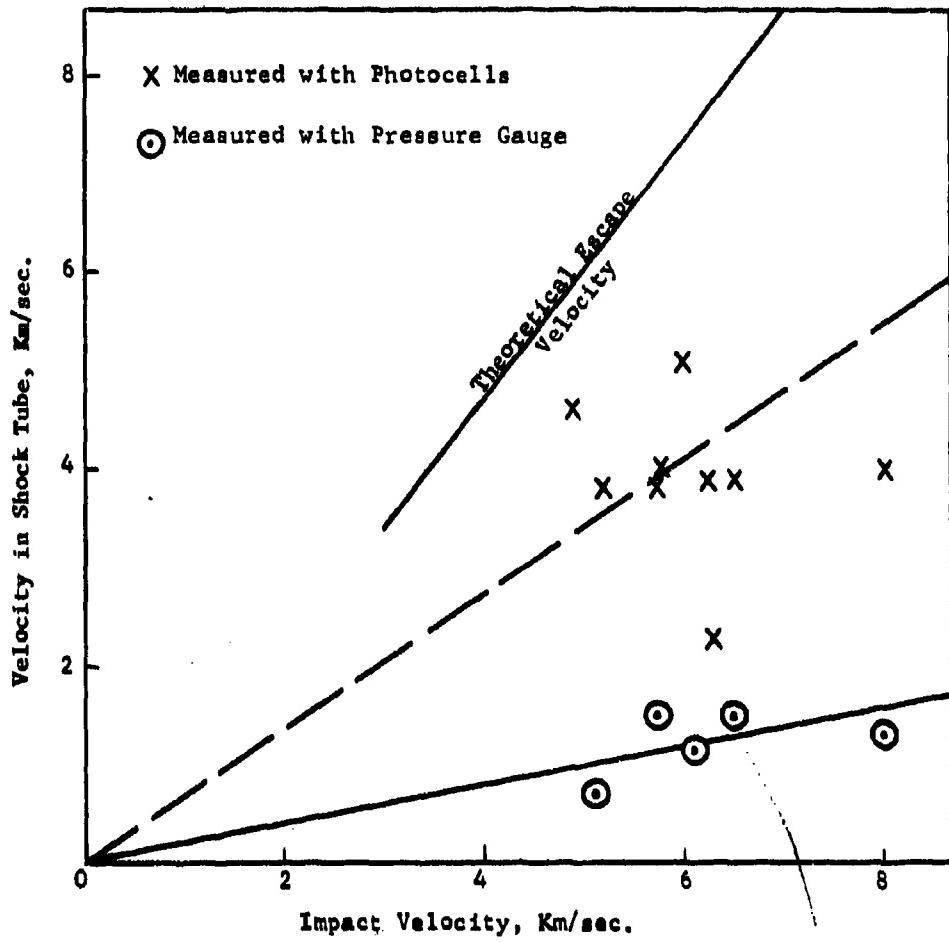
Figure 7 Velocities in Shock Tube
(Aℓ on Aℓ, 1 atm. O₂)
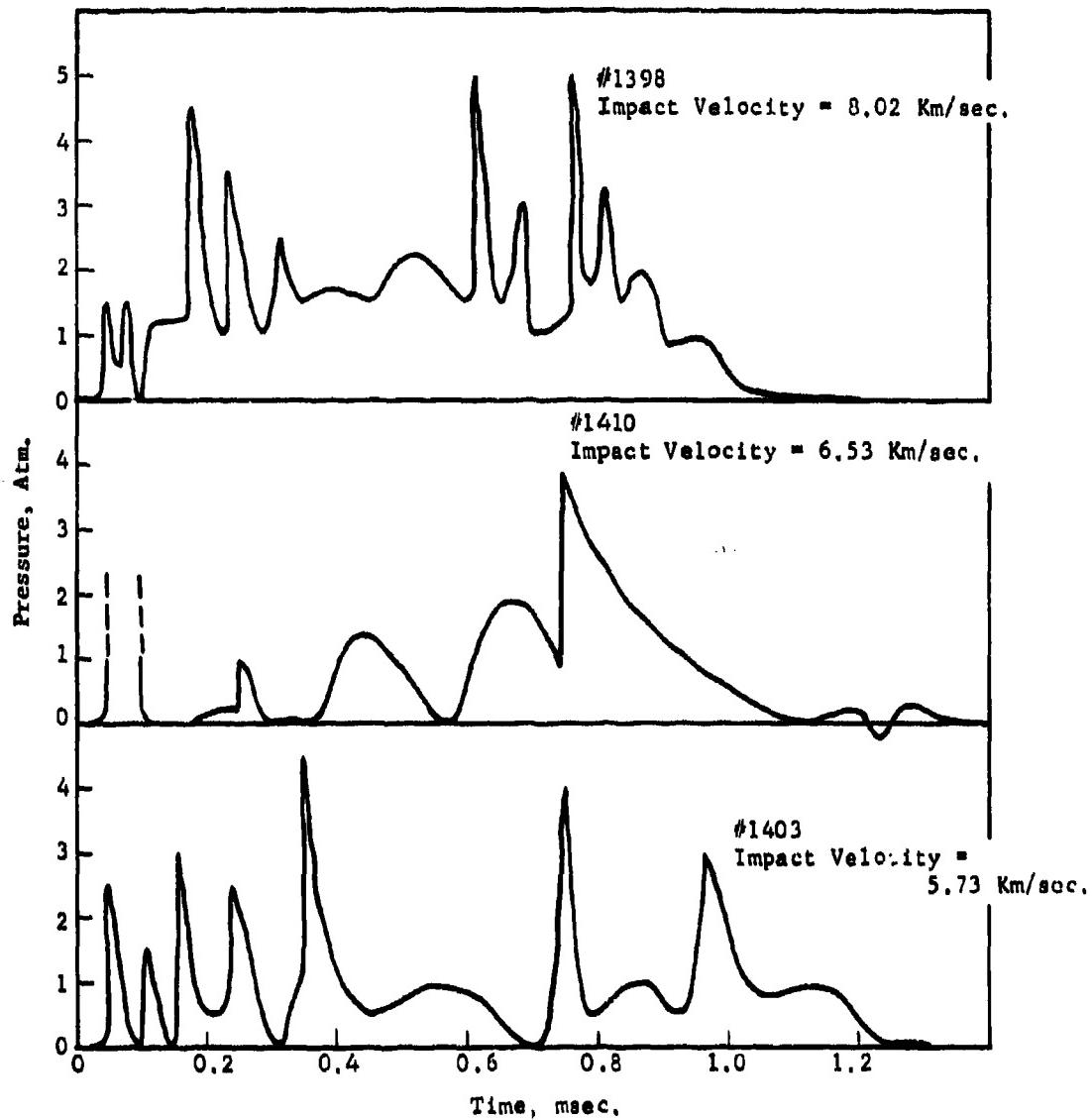
Figure 8 Typical Pressure Traces

(Al on Al, 1 atm. O₂)

front with a rapid exponential decay.

Initially, over the first 0.3 to 0.5 msec, at least two detonation waves seem to be generated near the target sheet. It is possible that the first detonation wave is born at some distance from the target sheet and that this incident wave is followed closely by a wave reflected off the target sheet.

It is also possible that several detonation waves are created initially since it would be expected that the oxidizing aluminum particles would not all explode at the same time because of the non-uniform particle size and temperature distribution. This is supported by the photocell traces which indicate that at least a few aluminum particles do reach the far end of the tube. It should also be added that in two instances where plastic witness sheets were placed in the rear of the shock tube, definite traces of molten aluminum were observed for impact velocities of 5.7 and 7.3 Km/sec.

According to the tentative calibration of the gauge, these initial pressure pulses reached values of 3 to 5 atmospheres. However, if it is assumed that the first detonation wave originated at impact at the target sheet and that oxygen behaves as a perfect polytropic gas, one can compute shock velocities (see Figure 7) which, in turn, will yield pressure values ranging from 5 to 21 atmospheres. Of course, since only one pressure gauge was used, the time and distance origin of the first detonation is not known. The average induction period of 40 μsec for the first pressure pulse is a long time with respect to the velocity of the aluminum fragments and, thus, the first detonation may well have originated at some appreciable distance downstream of the target sheet. However, it is believed that this distance must have been less than the length of the shock tube, 45.7 cm.

The initial detonation waves are followed generally by two late waves recorded from 0.6 to 0.9 msec after impact. It is possible that the first of these waves is a wave reflected off the rear of the shock tube which is again reflected off the target sheet, thus producing the second peak closely following the first (see Figures 9 and 10). This is supported by the fact that the time elapsed before recording the first of these two peaks corresponds approximately to the time that the very first wave would require to travel two shock tube lengths, if the shock velocities on Figure 7 are assumed correct. It should be remembered, however, that theoretically, a reflected shock should have a velocity lower than that of an incident wave and is subject to rapid attenuation.

It is also possible that the first of these two late peaks might have originated at the rear of the tube as a result of the oxidation of some of the remaining large aluminum fragments which impacted the wall at the rear of the shock tube. Such an impact would be expected to cause the aluminum to be much more reactive than after the original impact since the metal would be expected to reach a higher temperature and be more finely dispersed.

14
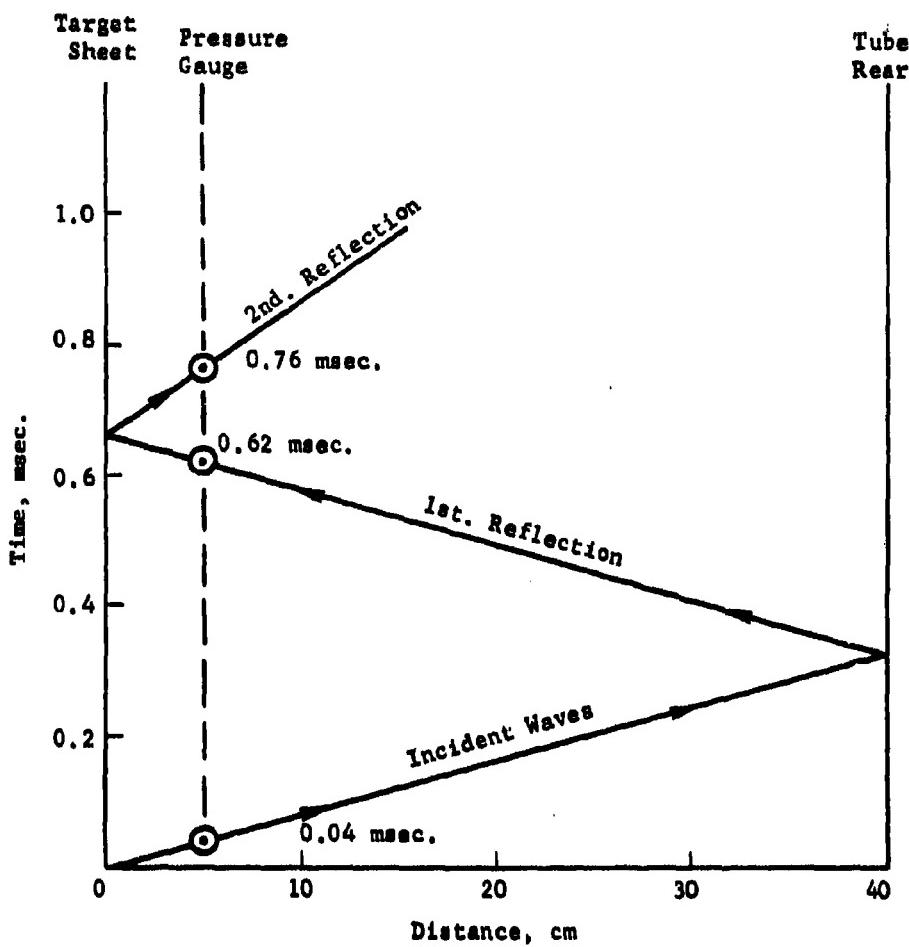
Figure 9   Possible Interpretation of a Pressure Trace
for Aℓ on Aℓ with 1 atm. O_2

(Shot #1398, Impact Velocity: 8.02 Km/sec)

A) Time elapsed before recording first incident pressure pulse

B) Time separation between the two "reflected" pressure peaks

C) Time elapsed before recording first "reflected" pressure peak
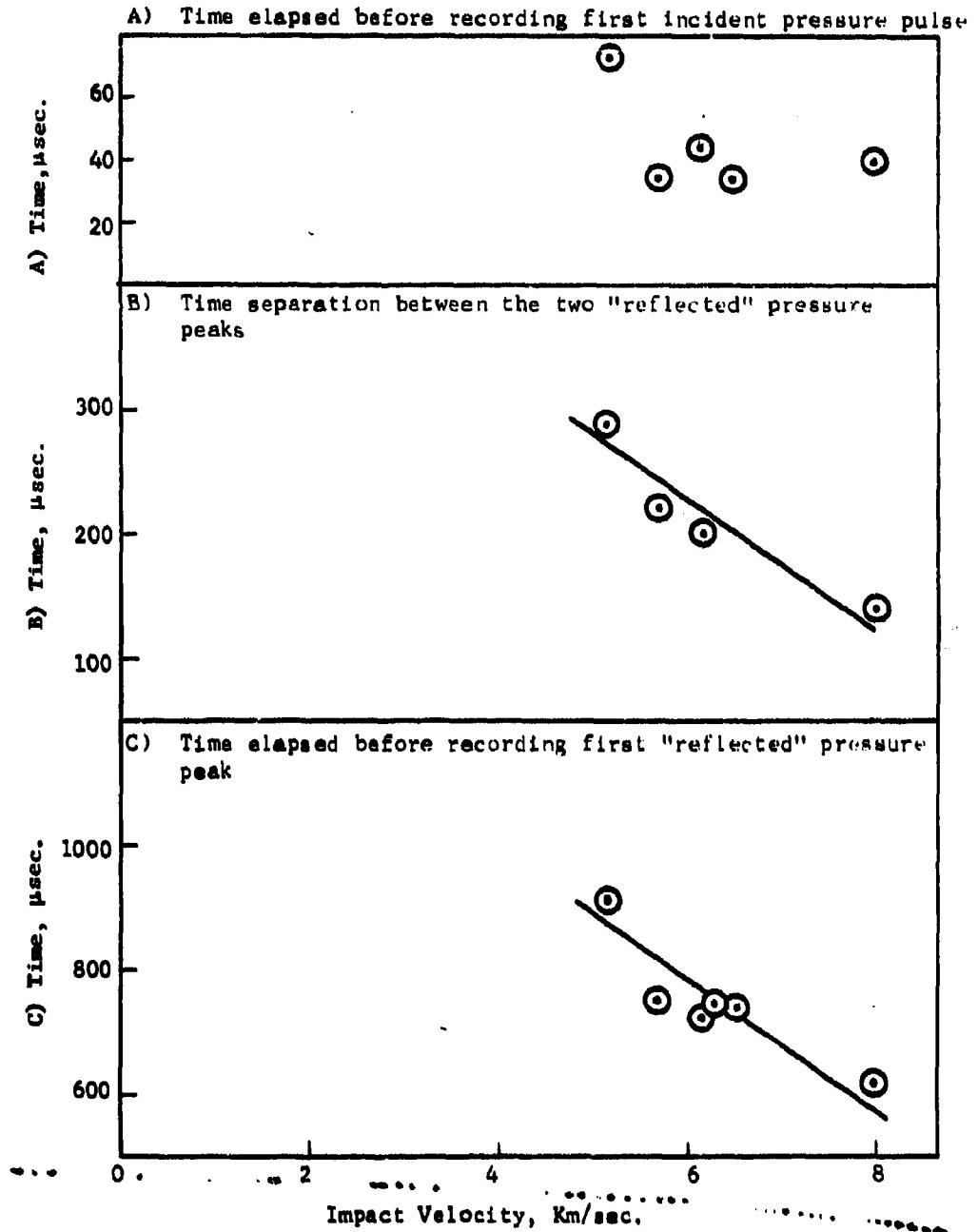
Figure 10   Pressure Trace Characteristics

(Al on Al, 1 atm. O_2)

16

Pressure traces were obtained for three cases where the target sheet did not burst and three where they did burst. All former three traces showed the two "reflected" peaks. However, among the three traces associated with the three burst sheets, one (impact velocity: 8.02 Km/sec) showed the two "reflected" peaks while the other two at lower velocities (6.53 and 6.31 Km/sec) showed only the first "reflected" pressure peak. It is thus tentatively concluded that the target sheets suffered the highest pressures when impacted by a detonation wave reflected off or originating at the rear of the shock tube and that, in one instance where the sheet blew out, the sheet collapse was slow enough to allow a wave reflection.

Attempts have been made to compute the pressures upon the target sheets associated with the "reflected" wave based upon the time separation between the last two pressure peaks and the gauge reading for the first of these two peaks (2 to 5 atm.); the values obtained are, however, not satisfactory (6 to 18 atm.). Instead, it is believed that the use of the standard equation for diaphragms should yield a more realistic value.

$$P = 4 t f_{ult.}/D$$

where P is the pressure difference across the diaphragm, t is the thickness of the diaphragm, D is the unsupported diameter, and $f_{ult.}$ is the ultimate tension stress (Reference 10). Assuming $f_{ult.}$ to have a value from 4 to 5.1 x 10^3 atm. (6.0 to 7.6 x 10^4 psi) one calculates bursting pressures of 55 to 65 atm. for the 0.25 and 0.30 mm target sheets, respectively. The above equation applies to unscored diaphragms subjected to static pressures; however, it is believed that the effect of the puncture in the target sheet should somewhat counterbalance the fact that the pressure is applied dynamically.

In conclusion, from the observation of the appearance of Al_2O_3, the bulges in the target sheets, the strong light intensities, and the traces of detonation waves, it appears that the shocked aluminum oxidized rapidly and more or less violently, depending upon the magnitude of the impact velocity.

C. Case II: Impact of Aluminum on Fiberglas Sheets Ret⁻ n at One Atmosphere

Three fiberglas sheets retaining oxygen at one impacted with aluminum spheres at velocities of 5.68, 6.28, a .

The following observations were made:

1. No cracks were observed following impact at 5. n/sec. At 6.28 Km/sec, the fiberglas was almost completely t around the edge of the supporting flange, and at 7.25 Km/sec the sheet burst and the epoxy charred along the edges of the large hole (see Figure 23, Appendix). Thus, it appears that the bursting velocity is approximately the same as for the case of the aluminum sheets (6.3 Km/sec).

17

2. As before, there is abundant evidence of the formation of what is believed to be Al_2O_3. Thus, it is clear that the projectile does participate in the oxidation reaction.

3. The recorded light signals differed from those obtained with the aluminum sheets (see Figure 11). The trace for the photocell nearest the target sheet shows considerably less light intensity and, in all three cases, shows two maxima where the second maximum (below saturation) occurs after 0.9, 1.4, and 1.4 msec have elapsed (the respective impact velocities are 5.68, 6.28, and 7.65 Km/sec). On the other hand, the traces of photocells #2, 3 and 4 were found to be essentially the same as in Case I.

   The difference in the first light trace might be caused by the fact that the first fragments of the expanding cloud are mainly glass which would not be expected to react appreciably with oxygen gas and which, therefore, would be expected to be less luminous. The glass particles might then temporarily protect the aluminum particles and lower the rate of oxidation for a few centimeters of travel distance.

   The resolution of the traces was too poor to calculate "escape" velocities but it may be stated that indications are that they were greater than the impact velocities. This increase over the values found for Case I is probably attributable to the different compressive properties of the fiberglas.

4. No pressure recordings were obtained for this series of three shots but the observation of two light intensity maxima, separated by about 1 msec near the target sheet, confirms the interpretation of the pressure history of Case I where a late detonation wave, originating at, or reflected off, the rear end of the shock tube, was believed responsible for the highest pressures suffered by the target sheet.

D. **Case III. Impact of Glass on a Fiberglas Sheet Retaining Oxygen at One Atmosphere**

A Pyrex sphere was impacted on a fiberglas sheet retaining oxygen at one atmosphere with a velocity of 6.00 Km/sec; unfortunately, an X-ray picture demonstrated that the projectile fractured before impact. Low level light intensity traces were observed in the shock tube even though the front face flash saturated the vacuum phototube for 400 μsec (see Figure 12).

Although there is no pressure record to show that detonations did not occur, it is very unlikely that a large scale exothermic reaction could have taken place in view of the chemical composition of the target and projectile. No doubt, some recombinations of ions and radicals with oxygen must have taken place, as well as some oxidation of the epoxy, but nothing on the scale of Case I. It is, however, quite possible that chemical effects might have been somewhat minimized by the fact that the glass projectile fractured in the barrel and thus the target may not have been shocked uniformly up to the anticipated impact pressure.

18
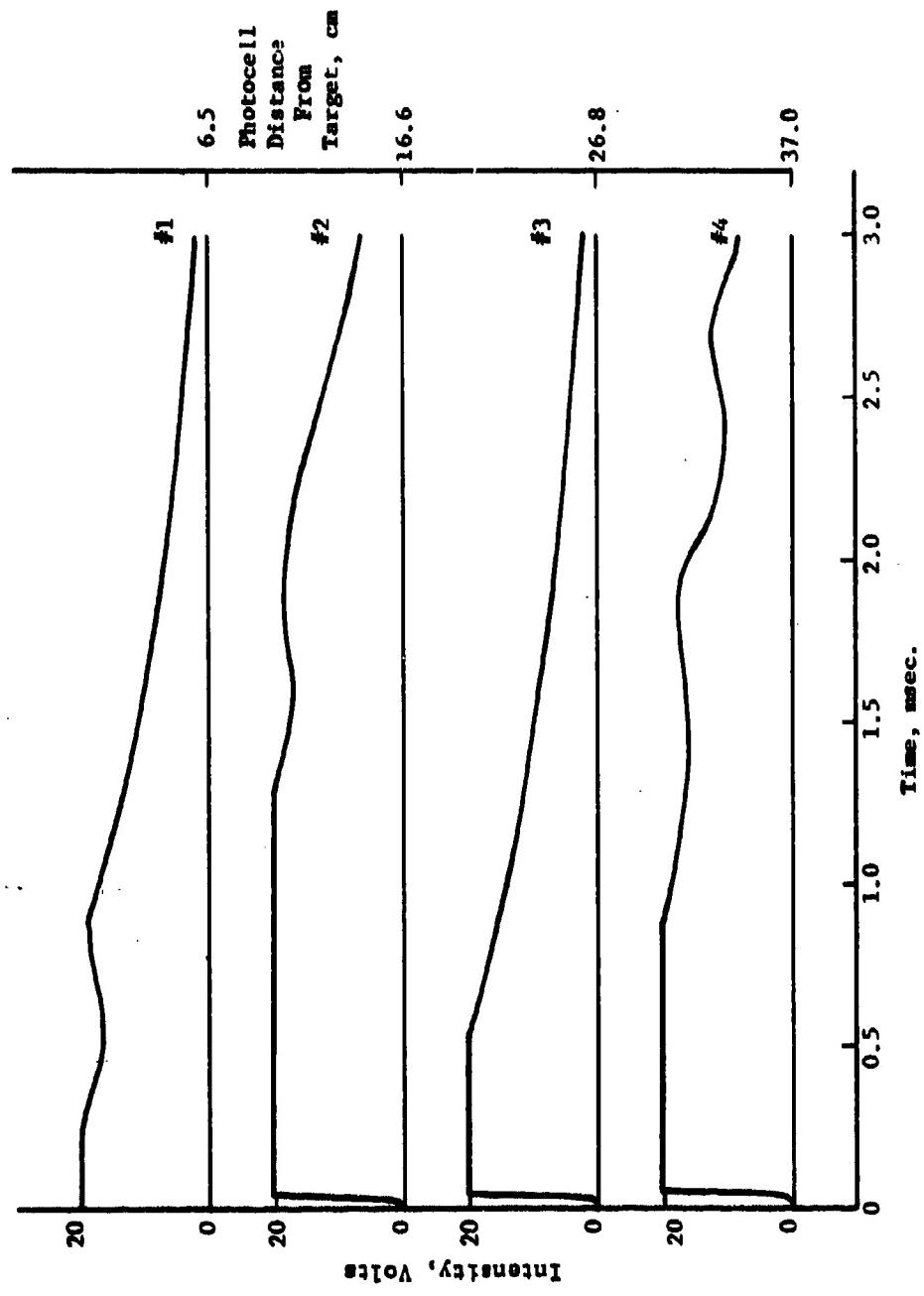
Figure 11 Typical Traces of Side Photocells for Aℓ on Fiberglas, 1 atm. O_2
(Shot #1387, Impact Velocity: 6.28 Km/sec)
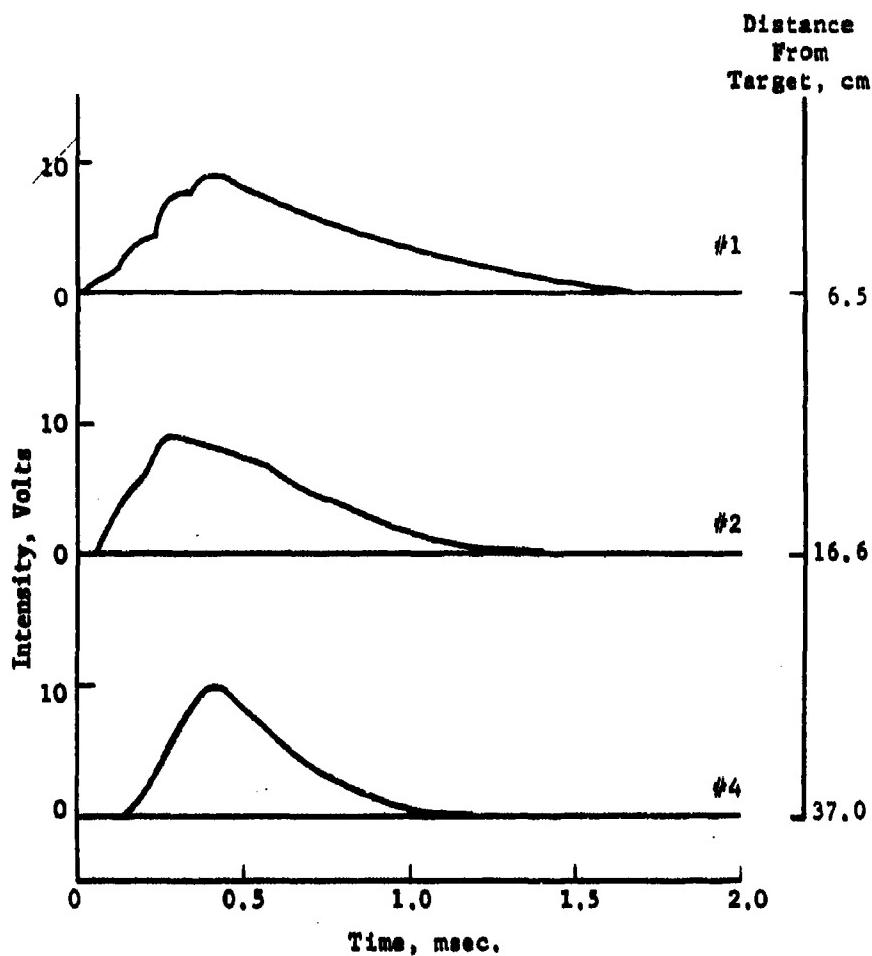
Figure 12 Traces of Side Photocells for Glass
on Fiberglas with 1 atm. O_2

(Shot #1390, Impact Velocity: 6.00 Km/sec)

E. **Case IV: Impact of Oxides on Aluminum Sheets Retaining Oxygen at One Atmosphere**

After observing that Pyrex projectiles fracture in the barrel, two other oxidized materials (single crystal quartz and a synthetic sapphire) were tested on aluminum targets retaining oxygen at one atmosphere. Unfortunately, they fractured again and hit the target as a spray of fine particles at velocities of 6.00 and 5.52 Km/sec, respectively.

For these two shots, only two photocell traces were recorded. In the case of the quartz impact, the intensity at photocell #1 went up to only half the saturation intensity (10 volts) while photocell #4 saw no light. Essentially the same traces were obtained from the sapphire impact except that the photocell nearest the target sheet did reach saturation for almost 0.9 msec. It thus appears that the impacted aluminum sheet (a small amount of metal as compared to an aluminum projectile) was rapidly exhausted through oxidation and did not survive the distance to the last photocell.

Only one pressure trace was recorded, that for the sapphire impact. It shows a single sharp narrow peak reaching 5 atmospheres 40 μsec after impact. Subsequently, the pressure rapidly reaches a low equilibrium value with no further disturbances. Again, it would seem that a small amount of aluminum reacted rapidly to completion and thus produced a small detonation wave which was attenuated rapidly. It is probable that larger detonations would have resulted had the projectiles not fractured because the target would have been more completely shocked; however, it would be expected that such detonations would still have been appreciably weaker than in Case I.

F. **Case V: Impact of Aluminum Spheres on Aluminum Sheets Retaining Helium at One Atmosphere**

Five aluminum sheets (0.25 mm thick) retaining helium at one atmosphere were impacted with aluminum spheres at velocities ranging from 3.35 to 7.07 Km/sec. Because of leaks in the shock tube and low pumping speed, about 0.1 atmosphere of air remained in the tube before filling with helium. Thus, it is estimated that the helium mixture included at least 2% oxygen.

For three shots at intermediate velocities (3.35, 4.39, and 5.24 Km/sec), the first three photocells recorded low light intensities while the fourth and remotest photocell recorded the strongest intensities which at the two higher velocities reached the saturation point (see Figure 13).

At a higher impact velocity (6.22 Km/sec) all photocells were saturated and the traces were similar to those obtained in Case I. In this instance, the aluminum sheet was extensively coated with a white powder believed to be Al_2O_3, and was near the bursting point: the bulge was pronounced and two cracks had radiated from the hole of the projectile (see Figure 24, Appendix).

For the last shot at the highest velocity (7.07 Km/sec) greater care was exercised in filling the shock tube with helium: the system was evacuated and filled with helium twice. Under those conditions, the aluminum sheet petalled outward and did show traces of Al_2O_3 (see Figure 24, Appendix). Photocell #4 quickly reached saturation but the traces for photocells #1
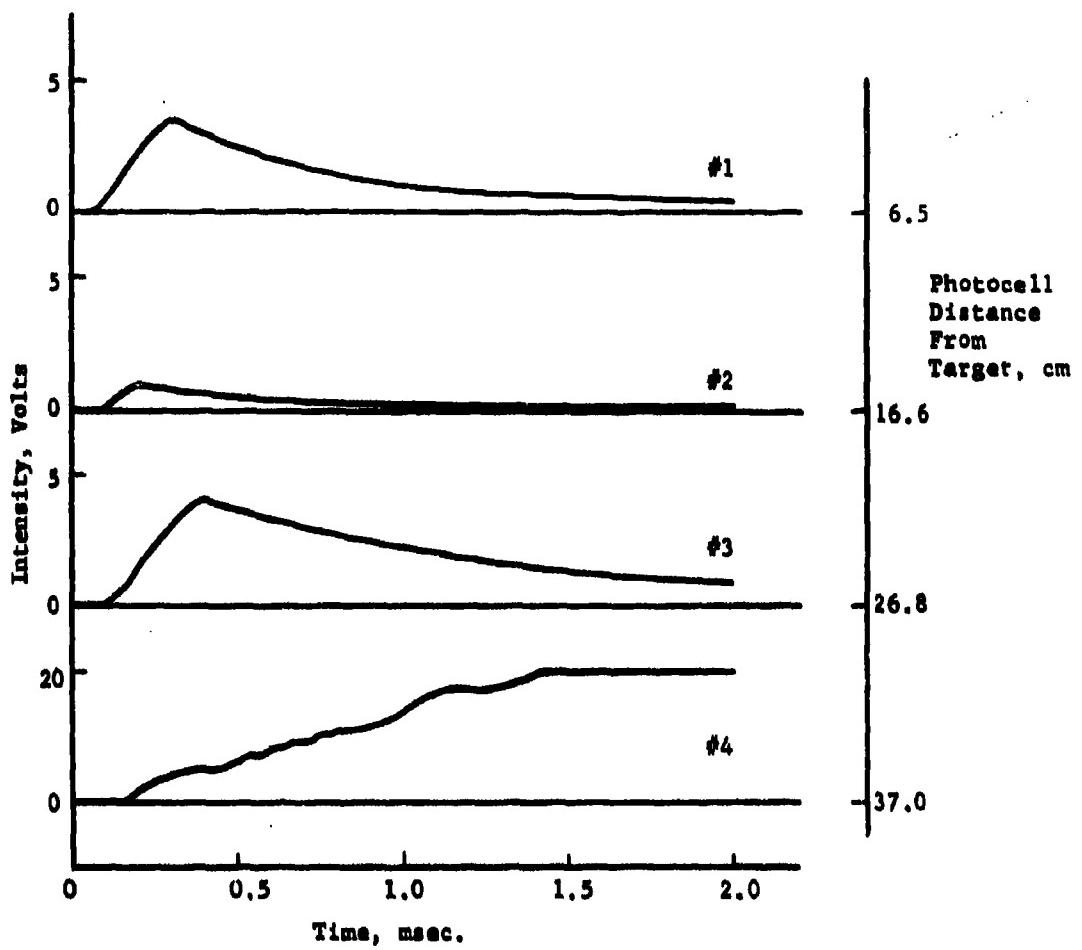
Figure 13   Traces of Side Photocells for Aℓ on Aℓ with 1 atm. He
(Shot #1380, Impact Velocity: 5.24 Km/sec)

and #3 showed an initial fairly slow rise to a value well below saturation
and, subsequently, a second rise to higher light intensity values (see
Figure 14) which caused saturation near the target sheet, approximately 0.5
to 0.6 msec after impact.

Although no pressure information was obtained for these experiments, it
may be surmised that 2% oxygen was sufficient to cause aluminum oxidation and
detonations. Certainly no reaction between helium and aluminum could take
place and it is unreasonable to believe that the strong pressures at the tar-
get sheet and the light in the shock tube were only caused by the transfer of
the impact pressure from the target sheet to the helium gas. In addition,
the total mass of shocked aluminum (projectile and target) represents 2.0 x
10^{-3} mole while the shock tube contained about 7 x 10^{-3} mole of oxygen. Thus,
there was about twice as much oxygen as is required for complete oxidation.

It is clear, however, that for the same impact velocity, a lower oxygen
concentration reduces the rate of oxidation and therefore the strength of
detonation waves. In addition, it is possible that the presence of helium
further lowers the reaction rates by acting as a heat dissipating medium.
Thus, in these instances, a large fraction of the aluminum particles must
have reached the end of the shock tube and impacted. In the process, the
aluminum was heated further and redispersed so that oxidation was suffi-
ciently facilitated to create detonation waves which then impinged upon the
target sheet.

G. **Case VI: Impact of Steel Spheres on Aluminum Sheets Retaining Oxygen
at One Atmosphere**

Five aluminum sheets (0.25 and 0.30 mm thick) were impacted with steel
spheres at velocities ranging from 4.89 to 5.81 Km/sec.

Traces for photocells #1 and #4 show considerable activity and satura-
tion was reached in all instances much as in Case I (see Figure 15). In
addition, there is abundant visible evidence of what is believed to be
Fe_2O_3 and Al_2O_3, and at 5.81 Km/sec the target sheet (0.30 mm thick) burst
(see Figure 23, Appendix). At a slightly lower velocity, 5.76 Km/sec, and
for the same thickness target sheet, 0.30 mm, two cracks were detected. It
is probable, however, that more cracks would have occurred if the hole area
in the target sheet had not been tripled by high velocity fiberglas debris.
Thus, it is concluded that the critical bursting velocity is very close to
5.8 Km/sec.

In two instances (impact velocity: 4.89 and 5.76 Km/sec), the traces of
photocell #4 showed long induction periods of 280 and 220 μsec, respectively.
These times correspond to velocities of 1.1 and 1.4 Km/sec which are too low
to represent fragment escape velocities but have the proper magnitudes for
shock wave velocities. This would imply that for these two shots the metal
cloud was not of sufficient luminosity to be observed. This is not altogether
unexpected since, for the same velocities, steel does not fragment as well
as aluminum and since iron is not as good a reducing agent as aluminum.

On the other hand, this explanation may not be of general validity in
the light of the same photocell traces for two other shots with impact

23
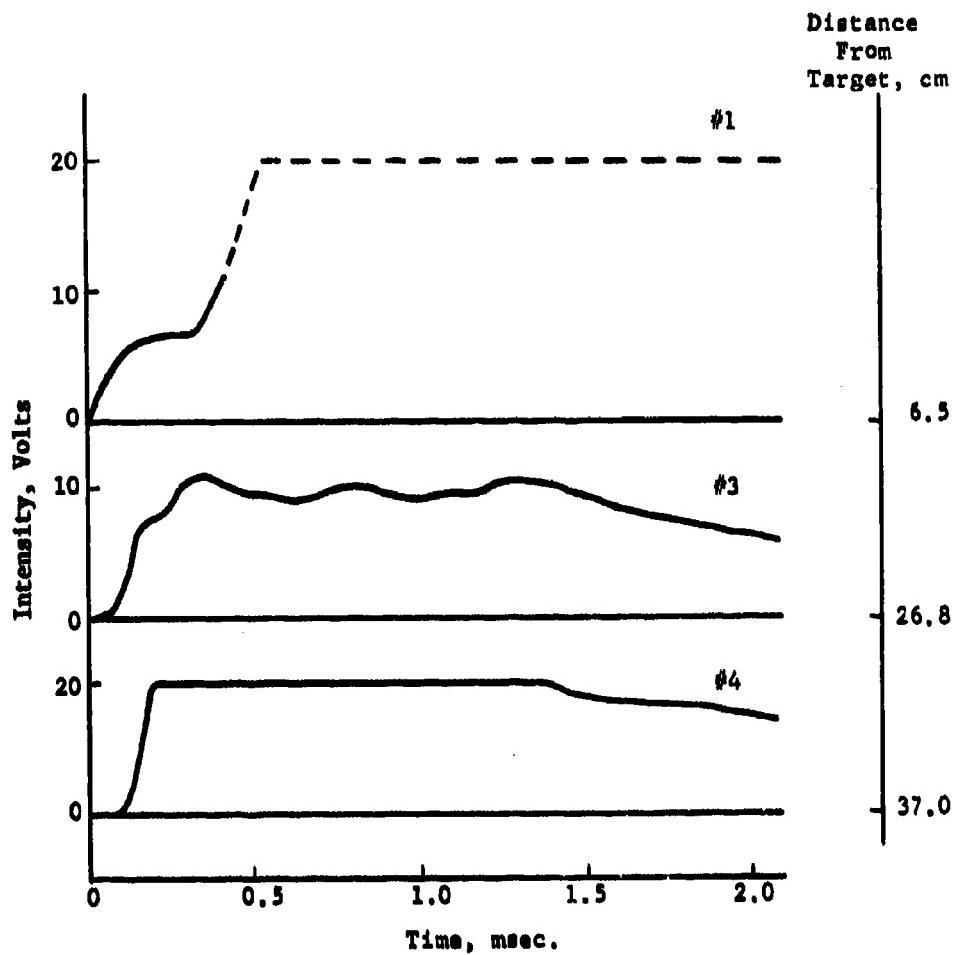
Figure 14   Traces of Side Photocells for
Al on Al with 1 atm. He

(Shot #1385, Impact Velocity: 7.07 Km/sec)

a) Shot #1441 (Impact Velocity: 5.81 Km/sec)
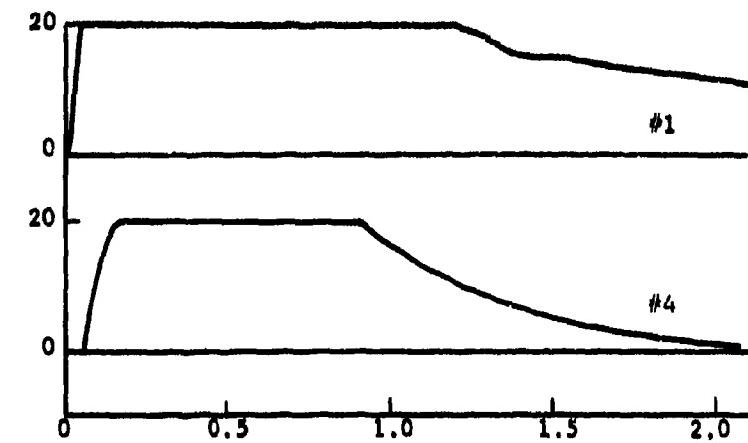
b) Shot #1406 (Impact Velocity: 4.89 Km/sec.)
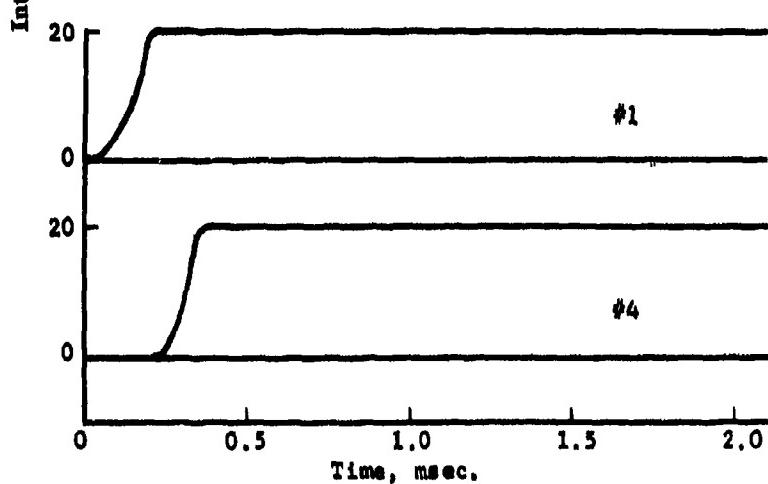
Figure 15 Traces of Side Photocells for Steel
on Aℓ with 1 atm. O_2

25

velocities of 5.17 and 5.81 Km/sec where much shorter induction periods (less than 100 μsec) were observed. It is, nevertheless, abundantly clear from the large splash of the lead on the target sheets originating from the rear plug of the shock tube that large solid fragments of steel survived the travel through the length of the tube.

Two good pressure traces were obtained (see Figure 16). Both show some initial detonation waves caused, no doubt, by the oxidation of the aluminum sheet. These were followed by other peaks the first of which occurred between 0.5 and 0.6 msec. Undoubtedly, this peak is responsible for bursting the target sheet since, for the case where the sheet burst, it was the last pressure peak while two more peaks followed when the sheet did not burst.

III. CONCLUSIONS

It is known from Rankine-Hugoniot data that following high velocity impacts both projectile and target reach high pressures and temperatures. Figures 17 through 19, prepared from published data (References 11 and 12), show that at 6 Km/sec the impact pressures and temperatures are 0.8 megabar (Mbar) and 2300°K for aluminum on aluminum and 1.2 Mbars, 2000°K, and 4100°K for iron on aluminum, respectively.

The shocked materials subsequently cool, expand, and fracture as a result of a rarefaction wave. This expansion is isentropic and involves the conversion of internal energy into kinetic energy. The final release temperatures after expansion in vacuum have been estimated by Bjork (Reference 13) for aluminum and are shown on Figures 18 and 19. Although the cooling is appreciable, it may be seen that at 6 Km/sec, aluminum is partly molten (930°K) and is liquid when impacted by aluminum and iron, respectively. Thus, in this velocity range, the release temperatures are fairly large and close to the ignition temperatures given in Table 1.

The oxidation, in the present range of impact velocities, undoubtedly occurs at the surface of the cloud particles and the heat released by the reaction will finally cause the particles to explode thus releasing gaseous metal which will react even faster and produce a detonation.

Our observations indicate that, for the range of velocities covered, detonations from aluminum oxidation start less than 40 μsec after impact and that the ensuing pressure disturbances caused by either the presence of aluminum alone or aluminum and steel with oxygen last from about 1.0 to 1.5 msec, depending upon the impact velocity. Apparently, strong detonations may be obtained with aluminum and oxygen pressures as low as 0.02 atm. There is also good evidence that organic materials such as epoxy polymers will react violently with oxygen following a high velocity impact.

It is clear, from our studies, that regardless of the impact velocity, and therefore the release temperature, so long as fresh metal surface is created by an impact, good reducing metals such as aluminum and iron will oxidize in the presence of oxygen. On the other hand, the strength of detonation waves is a function of (1) how much shocked metal and oxygen are available, (2) how much fresh metal surface (if the release temperature is below the boiling point) is created by the rarefaction wave in the target and

26
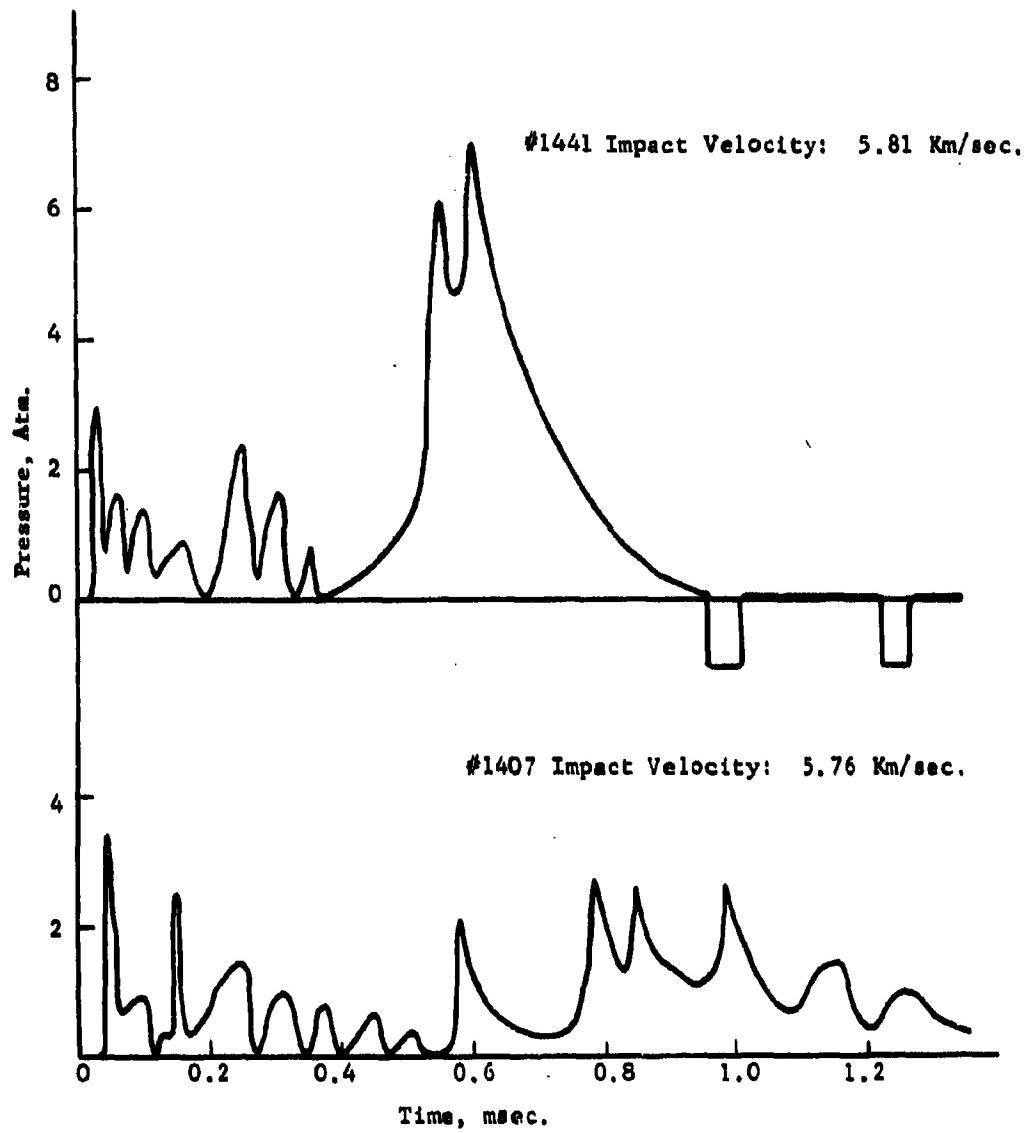
Figure 16 Pressure Traces

(Steel on Al, 1 atm. O_2)

27
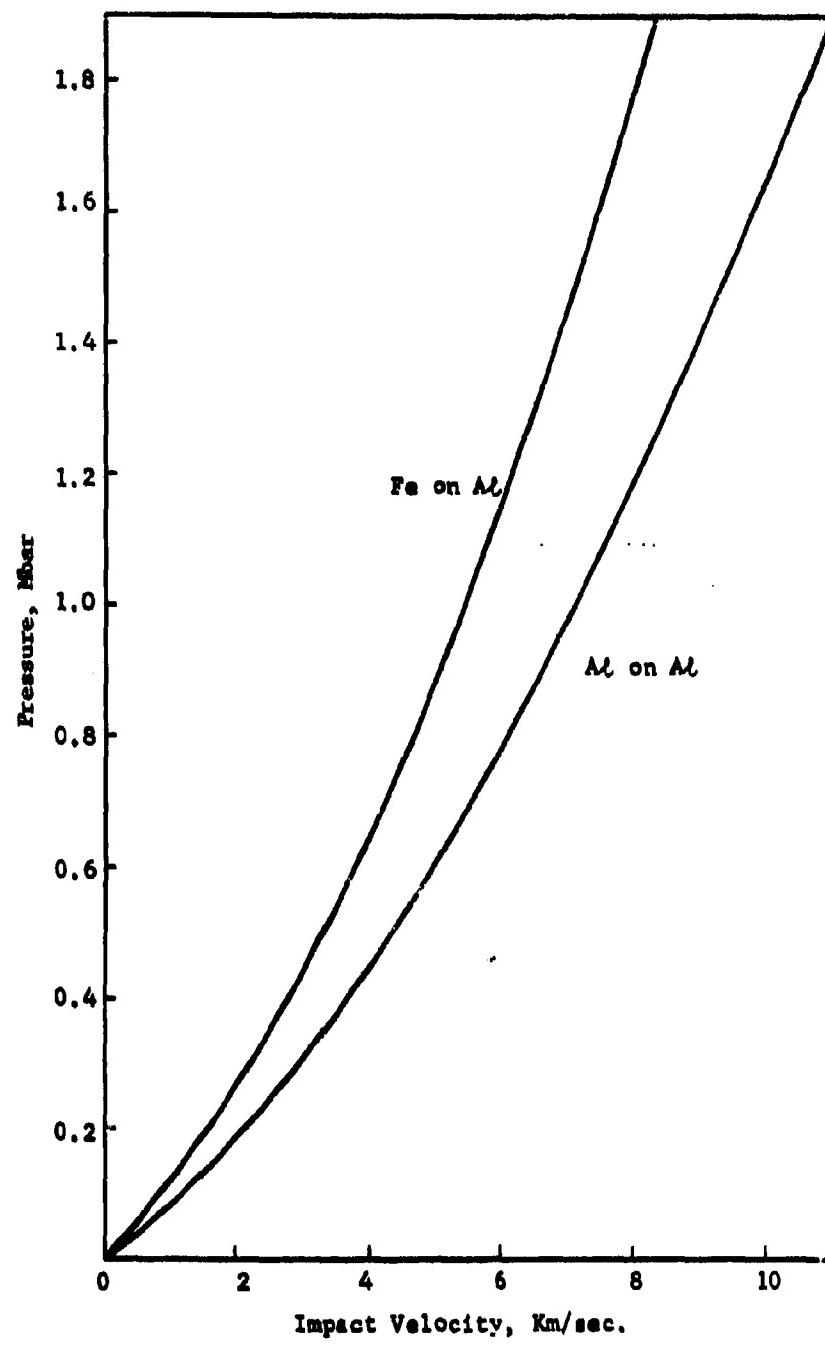
Figure 17 Hugoniot Impact Pressures
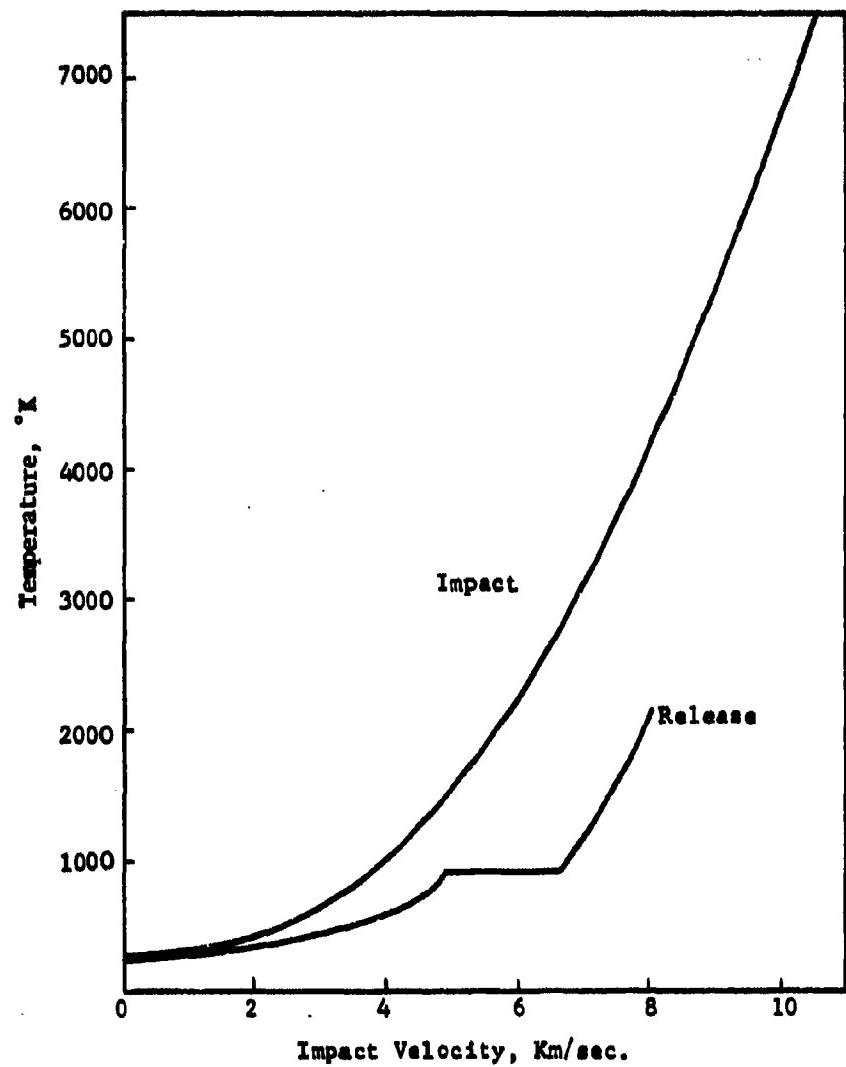
Figure 18   Temperatures for Aℓ on Aℓ Impacts

29
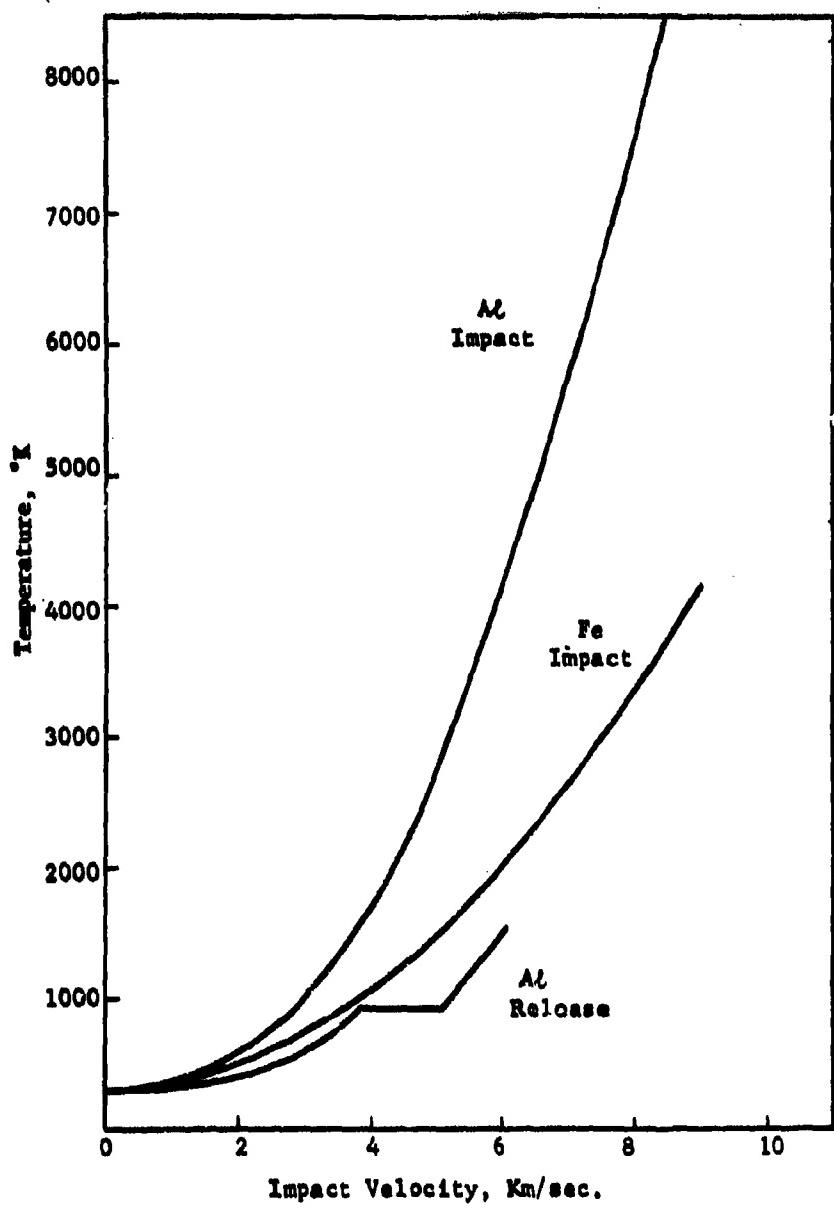
Figure 19 Temperatures for Fe on Al Impacts

projectile, (3) the release temperature and (4) the nature of the projectile and target. Thus the impact velocity, the ratio of the projectile diameter to the target thickness, and the relative compressive properties of the projectiles and targets are important factors since they will determine the release temperature, how well the impacted materials are dispersed after expansion, and what fraction of the shocked material will expand downstream of the target rather than upstream (Reference 7).

Clearly, our tests indicate that detonations from the oxidation of aluminum and steel may be quite large (55 - 65 atm.) in relation to the bursting strength of materials and at impact velocities which are quite modest compared to meteoroid velocities. This is not too surprising if one compares the kinetic energies at 6 Km/sec of an aluminum and a steel sphere (3.2 mm diameter), 0.82×10^{10} and 2.4×10^{10} ergs, respectively, with the heats of combustion at standard conditions, 1.7×10^{10} and 1.3×10^{10} ergs. No doubt, the shape of the shock tube did help to maximize the target sheet damage as the inside diameter was small enough to minimize the attenuation of the shock waves and the shortness of the tube brought about further fragmentation of the metal particles and/or the reflection of detonation waves.

Although it appears that in our tests none of the target sheets were burst by the first incident detonation wave, unquestionably, had the impact velocities been high enough to cause metal vaporization (about 10 to 12 Km/sec for aluminum on aluminum) this would not have been the case. Indeed, gaseous aluminum would be expected to react much more rapidly and violently with oxygen than solid or liquid aluminum. In such an event, a large detonation should take place very close to the target sheet and burst it within about 10 μsec without the necessity of wave reflection or particle impact at the rear wall of the tube. Thus, for the case of a meteoroid impacting a space vehicle with an average velocity of about 30 Km/sec, vaporization of the impacted wall should take place and therefore the damage to the wall would not be expected to be a function of the volume or dimensions of the space vehicle.

So far, no mention has been made of the chemical mechanisms which are responsible for the formation of the ultimate oxide products, Al_2O_3 and Fe_2O_3, which apparently have been obtained. This omission is only a reflection of the lack of data and in no way is it intended to convey the impression that it is a simple process. Within the range of experimental release temperatures encountered, it is quite probable that the initial oxidation products are Al_2O_3 and Fe_2O_3. However, as the temperature of the oxidizing metals rises, other products become thermodynamically favored (see Figure 20). Thus, aluminum has three oxides (Al_2O, Al_2O_2, and AlO) while iron has two oxides (Fe_3O_4 and FeO) which are known to be more stable than the usual oxides at high temperatures. Eventually, as the heat of the system is dissipated, these suboxides will be converted to the more familiar oxides.

There are a number of other factors which further complicates the kinetics of the oxidation process:

1. Not all metal particles of a given element will react at the same rate because of a distribution in particle size.

31
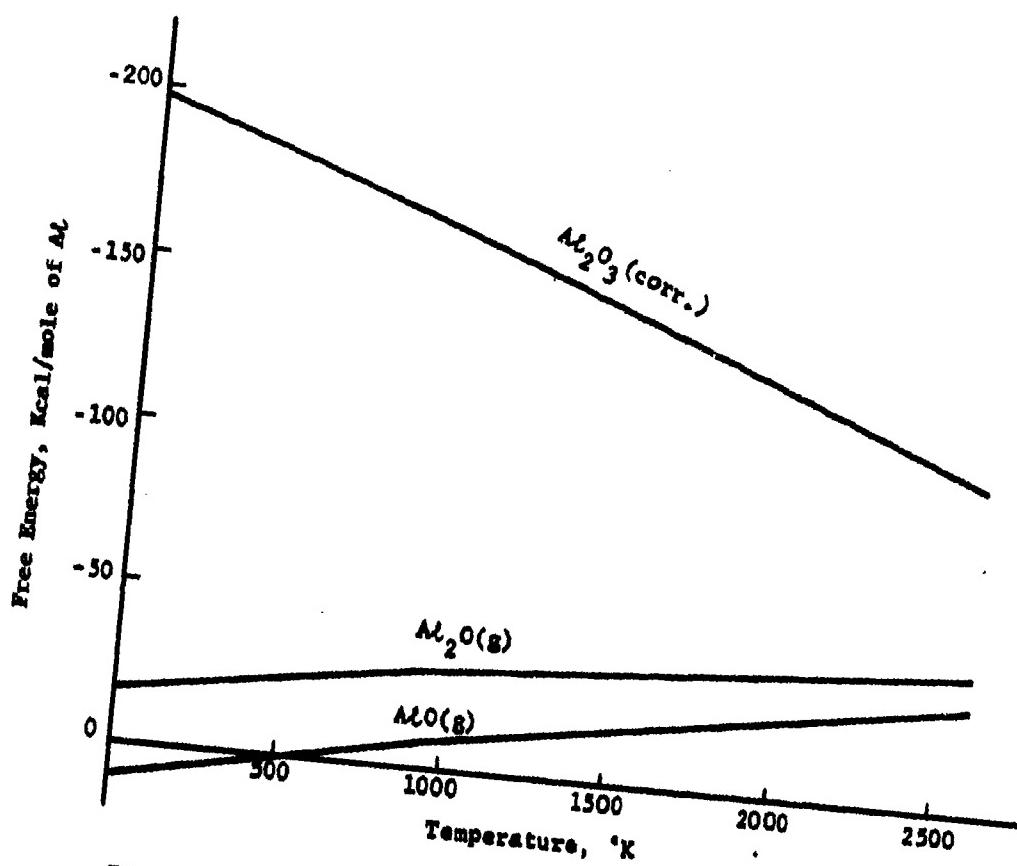
Figure 20   Free Energies of Formation for Aluminum Oxides
(Reference 14)

32

2. The temperature is changing rapidly and so are the reaction rates of the various chemical steps.

3. At the impact velocities encountered, the reacting aluminum or steel may react in three different phases: solid, liquid and gas.

4. The particles of the metal cloud are probably surrounded by a thin layer of shocked oxygen which should be initially at a much higher temperature and which might be appreciably dissociated.

IV. RECOMMENDATIONS

At this time, it is felt that oxidation detonations triggered by high velocity impacts have not been characterized in enough detail to ensure the full success of a study designed to prevent or attenuate the occurrence of such detonations. Instead, our original belief in the need for a systematic and fundamental investigation of this phenomenon has been reinforced by our preliminary observations.

A large body of theoretical and experimental work has been performed by Bull and co-workers (References 15, 7, 8, and 16) on the determination of the properties of expanding clouds resulting from impacts of cylinders with sheets in vacuum. It is felt that this work should be extended to spheres which are shaped more realistically, are easier to shoot, and are relatable to existing data. Such an investigation should include the study of impacts on sheets in vacuum, in an inert gas, such as helium, and, finally, in oxygen where an oxidation reaction would be anticipated. To this end, it would be preferable to use only one metal subject to oxidation in order to simplify the chemical mechanism. Aluminum for both the target and projectile is probably a good choice because high velocities are attained fairly easily.

Although the use of aluminum would allow the proper study of the expansion cloud with and without oxidation, there is little hope of attaining, in the laboratory, such velocities as are necessary to obtain complete vaporization. However, if the study of the expanding cloud per se is considered secondary, it might be possible to obtain true vaporization of the target sheet at impact in the laboratory at the expense of not properly fracturing and dispersing the projectile. Such a system would offer, nevertheless, the advantage of simpler kinetics (homogenous gaseous reactions) and would duplicate more nearly meteoroid impacts. The attainment of such conditions would require that the target sheet be made of a light element susceptible to oxidation with a low heat of sublimation, such as magnesium, and that the projectile be made of a heavy element not susceptible to oxidation, such as gold.

In order to analyze thoroughly the behavior of such systems, a number of properties would have to be determined:

1. Pressures at the target, in the expanding metal cloud, and at remote positions as a function of time.

2. The velocity of the expanding impacted material and of shock waves.

33

3. The temperature as a function of time and distance.

4. The shape of the expanding metal cloud as well as the mass and particle distribution in the metal cloud.

5. The location of the front of the rarefaction waves in the impacted materials as a function of time.

In addition, it would be of great interest to characterize the chemical species present as a function of time and to determine at what time the target is impacted by gaseous shock waves which may or may not cause bursting.

The instruments required to make such determinations are:

1. High speed cameras which have been developed to give 8×10^6 frames/sec.

2. Fast response quartz pressure gauges.

3. Fast response and high resolution vacuum phototubes which, with suitable filters, could be used to obtain information about the velocities of shock waves and particles, the chemical species present and temperatures as a function of time.

4. A visible and near-ultraviolet spectrograph to obtain a time-integrated record of the various chemical species formed.

5. Contact pins to follow the mechanical deformations of the target sheet as a function of time.

6. X-Ray diffraction equipment to characterize the compounds recovered from the tube walls and the target sheets after oxidative detonations.

34

REFERENCES

1) Rolsten, R. F., H. H. Hunt, and J. N. Willnitz, "Hypervelocity Impact on Pressurized Structures, Part I," AF 18(600)-1775, January (1962).

2) Rolsten, R. F. and H. H. Hunt, Astronautics and Aerospace Engineering, Vol. 1, No. 9, p. 20 (1963).

3) Thompson, A. B. and C. F. Gell, American Rocket Society Paper No. 2138-61, New York Coliseum, October (1961).

4) Gell, C. F., A. B. Thompson, and V. Stembridge, Aerospace Medicine, p 156, February (1962).

5) D'Anna, P. J., J. J. Piechocki, and A. Caron, "Self-Sealing Structures for Control of Meteoroid Hazard to Space Vehicles" (U), Part II (Confidential), NASr-102, March (1964).

6) MacCormack, R. W., "Impact Flash at Low Ambient Pressures," NASA TN D-2232, March (1964).

7) Bull, G. V., C. L. Murphy, F. Zwarts, and W. Friend, "Review of Hypervelocity Impact Studies at McGill University," Report No. 63-15, NASw-615, December (1963).

8) Friend, W. H., D. A. Millar, and C. L. Murphy, "The Hypervelocity Impact of Pellet with Thin Plates: Theoretical Considerations, Part II," Report No. 62-8, October (1962).

9) Nelson, L. S. and N. L. Richardson, J. Phys. Chem., 68, 1268 (1964).

10) Hall, J. G., University of Toronto Institute of Aerophysics Review No. 12, Part II, May (1958).

11) McQueen, R. G. and S. P. Marsh, J. Appl. Phys., 31, 1253 (1960).

12) Altshuler, L. V., S. B. Kormer, A. A. Bakanova, and R. F. Trunin, Soviet Physics JETP, 11, 573 (1960).

13) Bjork, R. L., Proceedings of the Sixth Symposium on Hypervelocity Impact, Vol. II, Part I, p. 1, August (1963).

14) Coughlin, J. P., Bureau of Mines, Bulletin 542 (1954).

15) Bull, G. V., "On the Impact of Pellets with Thin Plates," McGill TN 1-10/61 (1961).

16) Zwarts, F. J., "The Initial One-Dimensional Expansion of the Shocked States Generated by the Impact of Cylindrical Pellets with Thin Plates," NASA CR-54209, T.N. 64-6, January (1965).

APPENDIX

PHOTOGRAPHS OF A SELECTION OF

IMPACTED TARGET SHEETS

36
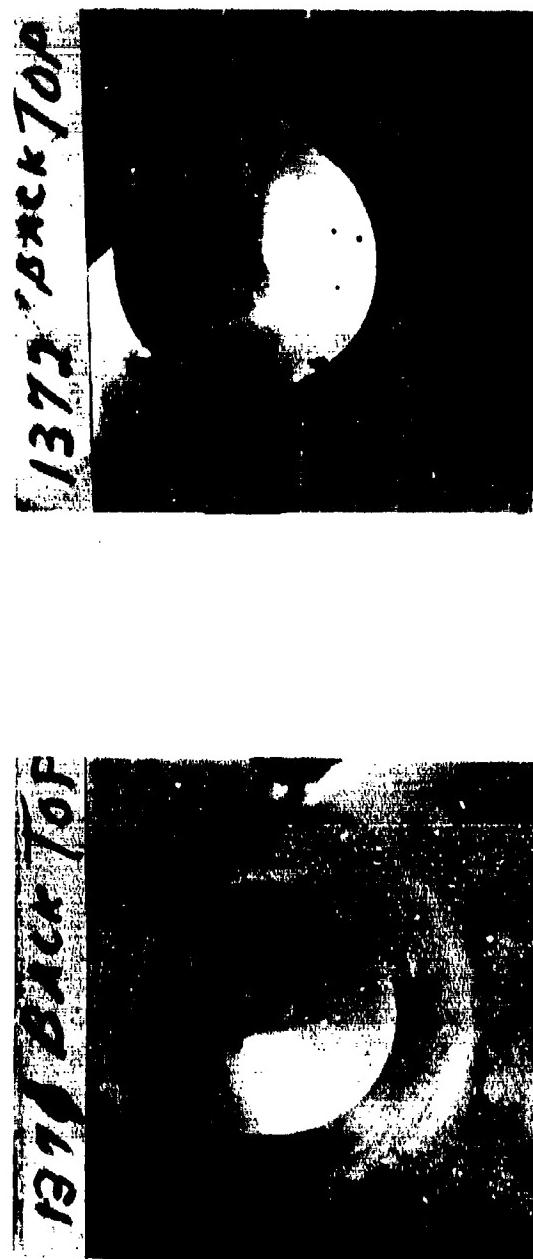
a) Shot #1371; impact velocity: 6.10 Km/sec; damage: small crack from projectile hole to neighboring debris hole (below projectile hole).

b) Shot #1372; impact velocity: 6.26 Km/sec; damage: small crack from projectile hole (to the right).

Figure 21 Case I Target Sheets After Impact
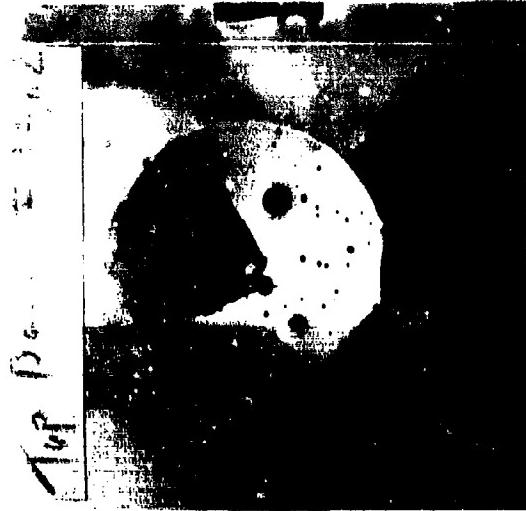
a) Shot #1412; impact velocity: 6.31 Km/sec; damage: bursting of target along the edges of the shock tube flange (projectile hole to the extreme center left).

b) Shot #1402; impact velocity: 6.16 Km/sec; damage: petalling originating at projectile hole

Figure 22 Case I Target Sheets After Impact

38
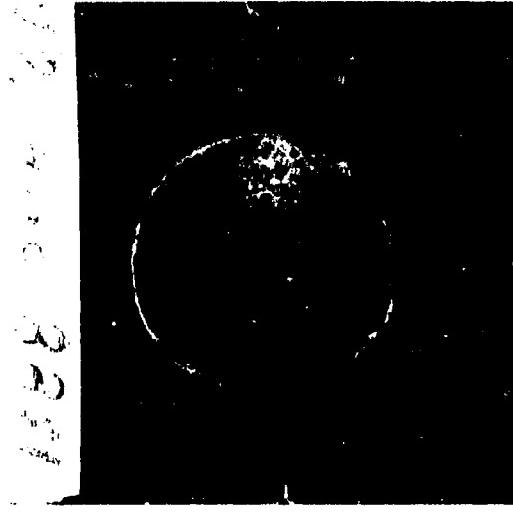
a) Case VI; Shot #1441, impact
velocity: 5.81 Km/sec; damage: bursting
of target (projectile hole in upper center).

b) Case II; Shot #1388; impact
velocity: 7.25 Km/sec; damage: bursting
of target with charring of epoxy.

Figure 23   Case II and VI   Target Sheets After Impact

1384 BackTop

1385 BackTop

a) Shot #1385; impact velocity: 7.07 Km/sec;
    damage: petalling originating at projectile
    hole.

b) Shot #1384; impact velocity: 6.22 Km/sec;
    damage: two cracks.

Figure 24 Case V Target Sheets After Impact

DOCUMENT CONTROL DATA - R&D

(Security classification of title, body of abstract and indexing annotation must be entered when the overall report is classified)

1. ORIGINATING ACTIVITY (Corporate author)	2a. REPORT SECURITY CLASSIFICATION
Air Force Flight Dynamics Laboratory Wright-Patterson AFB, Ohio	UNCLAS
	2b. GROUP

3. REPORT TITLE

Oxidative Detonations Initiated by High Velocity Impacts

4. DESCRIPTIVE NOTES (Type of report and inclusive dates)

Final Report

5. AUTHOR(S) (Last name, first name, initial)

Caron, A. P.

6. REPORT DATE	7a. TOTAL NO. OF PAGES	7b. NO. OF REFS
May 1965	44	16

8a. CONTRACT OR GRANT NO.	9a. ORIGINATOR'S REPORT NUMBER(S)
33(615)-2195	
b. PROJECT NO.	AFFDL TR 65-41
1469	
c.	9b. OTHER REPORT NO(S) (Any other numbers that may be assigned this report)
d.	NSL 65-50

10. AVAILABILITY/LIMITATION NOTICES US Government agencies may obtain copies of this report directly from DDC. Other qualified DDC users shall request through AF Flight Dynamics Laboratory, ATTN: FDTR, Keith I. Collier, WPAFB, Ohio.

11. SUPPLEMENTARY NOTES	12. SPONSORING MILITARY ACTIVITY
	AF Flight Dynamics Laboratory Wright-Patterson AFB, Ohio (FDTR)

13. ABSTRACT

Aluminum sheets (0.25 and 0.30 mm thick) retaining oxygen at one atmosphere have been observed to burst when impacted with steel and aluminum spheres (3.2 mm diameter) at velocities beyond 5.8 and 6.3 Km/sec, respectively. Visible deposits of aluminum and iron oxide, target sheet bulges, strong light intensities, and pressure gauge traces of detonation waves indicate that the bursting pressures were caused by the violent oxidation of steel and aluminum. Evidence of such reactions was detected over a wide range of impact velocities (4.88 to 8.02 Km/sec) and the violence of the reaction was found to be a function of the velocity. Other tests showed that both the projectile and the target participate in the formation of detonations and that other factors determining the strength of such detonations are the concentration of oxygen and the amount of impacted metal susceptible to oxidation.

DD FORM 1 JAN 64 **1473**

14. KEY WORDS	LINK A		LINK B		LINK C	
	ROLE	WT	ROLE	WT	ROLE	WT

INSTRUCTIONS

1. ORIGINATING ACTIVITY: Enter the name and address of the contractor, subcontractor, grantee, Department of Defense activity or other organization (*corporate author*) issuing the report.

2a. REPORT SECURITY CLASSIFICATION: Enter the overall security classification of the report. Indicate whether "Restricted Data" is included. Marking is to be in accordance with appropriate security regulations.

2b. GROUP: Automatic downgrading is specified in DoD Directive 5200.10 and Armed Forces Industrial Manual. Enter the group number. Also, when applicable, show that optional markings have been used for Group 3 and Group 4 as authorized.

3. REPORT TITLE: Enter the complete report title in all capital letters. Titles in all cases should be unclassified. If a meaningful title cannot be selected without classification, show title classification in all capitals in parenthesis immediately following the title.

4. DESCRIPTIVE NOTES: If appropriate, enter the type of report, e.g., interim, progress, summary, annual, or final. Give the inclusive dates when a specific reporting period is covered.

5. AUTHOR(S): Enter the name(s) of author(s) as shown on or in the report. Enter last name, first name, middle initial. If military, show rank and branch of service. The name of the principal author is an absolute minimum requirement.

6. REPORT DATE: Enter the date of the report as day, month, year; or month, year. If more than one date appears on the report, use date of publication.

7a. TOTAL NUMBER OF PAGES: The total page count should follow normal pagination procedures, i.e., enter the number of pages containing information.

7b. NUMBER OF REFERENCES: Enter the total number of references cited in the report.

8a. CONTRACT OR GRANT NUMBER: If appropriate, enter the applicable number of the contract or grant under which the report was written.

8b, 8c, & 8d. PROJECT NUMBER: Enter the appropriate military department identification, such as project number, subproject number, system numbers, task number, etc.

9a. ORIGINATOR'S REPORT NUMBER(S): Enter the official report number by which the document will be identified and controlled by the originating activity. This number must be unique to this report.

9b. OTHER REPORT NUMBER(S): If the report has been assigned any other report numbers (*either by the originator or by the sponsor*), also enter this number(s).

10. AVAILABILITY/LIMITATION NOTICES: Enter any limitations on further dissemination of the report, other than those imposed by security classification, using standard statements such as:

(1) "Qualified requesters may obtain copies of this report from DDC."

(2) "Foreign announcement and dissemination of this report by DDC is not authorized."

(3) "U. S. Government agencies may obtain copies of this report directly from DDC. Other qualified DDC users shall request through

_____."

(4) "U. S. military agencies may obtain copies of this report directly from DDC. Other qualified users shall request through

_____."

(5) "All distribution of this report is controlled. Qualified DDC users shall request through

_____."

If the report has been furnished to the Office of Technical Services, Department of Commerce, for sale to the public, indicate this fact and enter the price, if known.

11. SUPPLEMENTARY NOTES: Use for additional explanatory notes.

12. SPONSORING MILITARY ACTIVITY: Enter the name of the departmental project office or laboratory sponsoring (*paying for*) the research and development. Include address.

13. ABSTRACT: Enter an abstract giving a brief and factual summary of the document indicative of the report, even though it may also appear elsewhere in the body of the technical report. If additional space is required, a continuation sheet shall be attached.

It is highly desirable that the abstract of classified reports be unclassified. Each paragraph of the abstract shall end with an indication of the military security classification of the information in the paragraph, represented as (*TS*), (*S*), (*C*), or (*U*).

There is no limitation on the length of the abstract. However, the suggested length is from 150 to 225 words.

14. KEY WORDS: Key words are technically meaningful terms or short phrases that characterize a report and may be used as index entries for cataloging the report. Key words must be selected so that no security classification is required. Identifiers, such as equipment model designation, trade name, military project code name, geographic location, may be used as key words but will be followed by an indication of technical context. The assignment of links, rules, and weights is optional.